Aus der Abteilung für Klinische Pharmakologie

Direktor: Prof. Dr. med. Stefan Endres

Medizinische Klinik und Poliklinik IV

Klinik der Ludwig-Maximilians-Universität München

Direktor: Prof. Dr. med. Martin Reincke

T cell receptor modification by alpha and beta chain domain cross-over for adoptive T cell therapy

Dissertation

zum Erwerb des Doktorgrades der Medizin

an der Medizinischen Fakultät der

Ludwig-Maximilians-Universität zu München

vorgelegt von

Philipp Konstantin Peters

aus München

2018

Mit Genehmigung der Medizinischen Fakultät

der Universität München

Berichterstatter:	Prof. Dr. med. Stefan Endres
Mitberichterstatter:	Prof. Dr. med. Tobias Feuchtinger
	Prof. Dr. med. Marion Subkleve
Mitbetreuung durch den promovierten Mitarbeiter:	PD Dr. med. Sebastian Kobold
Dekan:	Prof. Dr. med. dent. Reinhard Hickel
Tag der mündlichen Prüfung:	08.11.2018

Table of contents

1 Zusammenfassung

Adoptiver T-Zelltransfer ist ein Therapieverfahren, bei dem Patienten-eigene T-Lymphozyten mit einem tumorspezifischen Rezeptor transduziert werden, um eine anti-tumorale Aktivität zu induzieren

Trotz vieler Fortschritte birgt dieses Verfahren auch Risiken. Eines ist die Bildung autoreaktiver T-Zellen: Die Erkennungsdomäne des T-Zellrezeptors ist ein Dimer aus α- und β-Kette. Daher kann, durch Hinzufügen eines zweiten T-Zellrezeptors in eine T-Zelle, ein weiteres Dimer aus einer nativen und einer exogenen Kette entstehen. Ein solcher, fehlgepaarter (’mispaired’) Rezeptor kann potenziell neue Antigene erkennen und Autoimmunreaktionen auslösen.

Gegenstand der vorliegenden Arbeit ist es eine neuartige T-Zellrezeptormodifikation zum Unterbinden von Mispairing zu untersuchen. Dazu vertauschten wir die konstante oder die variable Domäne zwischen den Ketten (’domain crossover’). Dieses Prinzip wird bereits erfolgreich beim Design von bispezifischen Antikörpern eingesetzt, um Mispairing zu vermeiden und könnte sich dank großer Homologie auf T-Zellrezeptoren übertragen lassen.

Bei Transduktion der gekreuzten Rezeptorketten in murine T-Zellen, stellten wir zunächst keine Oberflächenexpression, jedoch eine intrazelluläre Akkumulation von gekreuzten α-Ketten fest. Nach Beseitigung einer Interferenz durch die Linkersequenz stellte sich eine temporäre Oberflächenexpression der α-Kette des gekreuzten Rezeptors ein. Transduzierten wir jedoch nur eine einzelne Kette, so war keine Oberflächenexpression nachweisbar. Wir folgerten, dass auch die grundsätzlich nicht mehr detektierbare β-Kette exprimiert wird und sich gekreuzten Ketten erfolgreich mit CD3 Untereinheiten zusammensetzen.

Um eine stabile Oberflächenexpression zu ermöglichen, fügten wir Disulfidbrücken ein und veränderten die genaue Kreuzungsstelle innerhalb der Ellbogenregion, welche die variable und konstante Domäne verbindet. Es ließ sich jedoch keine dauerhafte Oberflächenexpression erzielen. Somit sind andere Strategien erforderlich um Mispairing zu verhindern oder zu reduzieren.

2 Abstract

Adoptive T cell transfer is a novel approach for cancer treatment in which patient's T lymphocytes are extracted and genetically modified to redirect these against the cancer cell.

However, there are still a number of risks and limitations to this approach. One is the formation of autoreactive T cell: The antigen-recognizing part of the T cell receptor is a dimer of an α- and a β-chain. Accordingly, transduced T cells can express 'mispaired' T cell receptors that comprise a native and an exogenous chain. These heterodimers can cause autoimmunity if they target self-antigens.

The aim of this study was to investigate a novel approach against mispairing by transferring either the variable or the constant domain of one chain across to the other chain. This concept is already successfully employed in the design of bispecific antibodies to avoid mispairing and may be transferable due to a high degree of homology between T cell receptors and antibodies.

The transduction of crossed receptors into murine T cells did not result in any surface expression. We observed an intracellular accumulation of α-chains. After a redesign eliminating an interference with the linker sequence, we found a temporary surface expression of α-chains in one of our constructs. However, when transducing only the single chain, we could not detect surface expression. We concluded that, while undetectable, the β-chain must be expressed when transducing with the bicistronic vector and that the crossed T cell receptor assembles correctly with the CD3 subunits.

Finally, we aimed at stabilizing surface expression of the crossed receptor. We added an additional disulfide bond between both chains at different locations and changed the exact location of the domain cross-over in the so-called elbow region, which links the variable and the constant domain of each chain. Yet, a sustained surface expression of crossed T cell receptors could not be achieved. Alternative strategies are thus needed to prevent TCR mispairing.

3 Introduction

3.1 Cancer immunotherapy

Adoptive cell therapy (ACT) is a highly promising, however not yet approved form of cancer immunotherapy (Pedrazzoli et al. 2012). In ACT, tumor-specific cytotoxic T cells are expanded and stimulated *in vitro* to elicit an antitumoral response upon reinfusion to the patient. Clinical studies have shown the efficacy of this approach even in patients with advanced and refractory disease (Rosenberg et al. 1988, Dudley et al. 2002)

In clinical studies, two main approaches are employed to generate the required T cell population: Isolating and expanding pre-existing tumor-specific lymphocytes *ex vivo* or genetic modification of T cells that are initially not tumor-reactive (Pedrazzoli et al. 2012). The former relies on isolation of tumor-infiltrating lymphocytes (TIL) out of tumorous tissue (Wu et al. 2012) - a process which is considered a critical limitation to TIL-based ACT, as many tumor entities do not possess sufficiently many TIL to allow for *ex vivo* extraction (Restifo et al. 2012). This limitation is overcome by the latter approach: In gene transfer-based ACT (gtACT), patients' T cells are genetically engineered to become tumor-reactive. This is commonly achieved by either transferring a tumor-specific TCR or a chimeric antigen receptor (CAR), directing cytotoxic T cells towards the tumor (Sadelain et al. 2003, Hughes et al. 2005).

However, both forms of ACT share other considerable limitations regarding effectiveness and safety. As ACT critically depends on antigen recognition and T cell activation, tumors that impair either of these pillars can escape an effective T cell response: Tumors can circumvent antigen recognition by either loss of target antigens (Maeurer et al. 1996) or a downregulation of major histocompatibility complex class I expression (MHC I) (Ferrone et al. 1995, Restifo et al. 1996). Also, it has been shown that a variety of tumors create an immunosuppressive milieu by soluble and membranous molecules such as

transforming growth factor β (TGFβ) or programmed death ligand 1 (PD-L1) (Dougan et al. 2009), as well as recruitment of immune-regulatory cells like regulatory T cells (Treg) (Antony et al. 2005) or myeloid derived suppressor cells (MDSC) (Payne et al. 2012). In solid tumors, poor access to the cancerous compartment, leading to “immunological ignorance” is also considered a relevant hurdle to an efficient anti-tumoral T cell response (Ochsenbein et al. 1999).

Some of these limitations can be addressed by a lymphodepleting pretreatment, which has significantly increased the initial response rate up to 72% and has even resulted in long-term regressions (Dudley et al. 2008, Rosenberg et al. 2011). Lymphodepletion, either by total body irradiation (TBI) or chemotherapy, is thought to enhance ACT by the following mechanisms: For one, it creates a niche in lymphatic organs and bone marrow for transferred T cells to proliferate and persist (Dudley et al. 2002). Secondly, it decreases the number of immunosuppressive cells fostering a stronger antitumoral response (Gattinoni et al. 2005, Kmieciak et al. 2011). And finally, it is believed, that the induced tissue damage leads to the release of proinflammatory cytokines, which in turn attract immune cells to the location of the tumor (Payne et al. 2012).

Yet, safety concerns remain: The two most important dangers are the creation of autoreactive T cells and the malignant degeneration of the infused lymphocytes. While the first is usually explained by off-target reactivity causing damage to healthy tissue and a potentially lethal “cytokine storm” (Schumacher 2002, Riechelmann et al. 2007), the latter is due to the highly active viral promoters, randomly inserted into the cells genome, potentially activating oncogenes or causing insertional mutagenesis (Woods et al. 2003). When contemplating the risk of autoreactive T cells in gtACT, the main consideration is the target antigen. It requires careful selection and extensive research to choose an antigen which is expressed on as many cancer cells as possible, but at the same time remaining specific.

3.2 T cell receptor mispairing

Even with the most careful selection of cancer antigen, the danger of self-reactivity cannot be completely contained in gtACT. This is due to the structure of the TCR: The TCR is a multimer, comprising a heterodimer of two chains, the alpha (TCRα) and the beta (TCRβ) chain, which together recognize an antigen fragment in the context of a MHC-I molecule. When transducing a T cell with a cancer specific TCR, the expression of the endogenous TCR is unaffected. Hence, a transduced T cell expresses two different TCRα and TCRβ chains each. However, these four proteins cannot only form two functional TCR, but four: Next to an all-endogenous and an all-exogenous TCR, two further TCR can form by heterodimerization of an endogenous and an introduced chain. It was long hypothesized that these mispaired TCR (often referred to as heterodimeric TCR) could potentially recognize MHC-I coupled self-antigens (Merhavi-Shoham et al. 2012), even when neither the endogenous, nor the introduced TCR would do so (Figure 1).

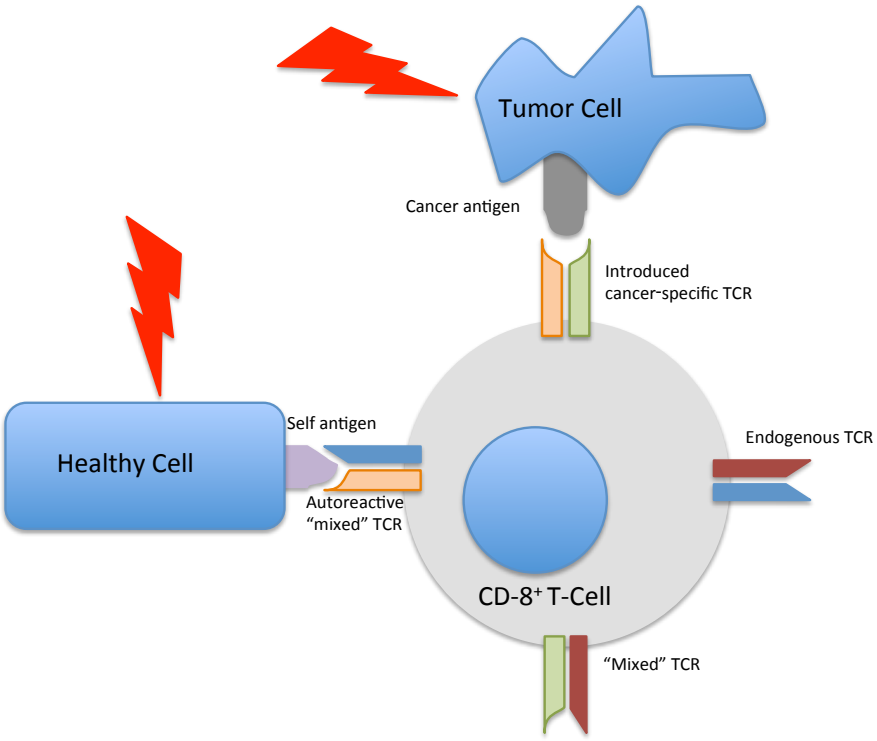

Figure 1: T cells transduced with a cancer-specific TCR can become autoreactive: Even though neither the original (right), nor the introduced TCR (top) recognize self-antigens, T cells can attack healthy cells because of mispaired TCR chains (left and bottom) (Engels et al. 2007).

For a long time, this effect has been a subject of discussion as – though in theory plausible – it was never directly proven. In 2010 Bendle et al. brought forward compelling evidence that mispairing can cause severe toxicity in a mouse model. Their group described an effect, which they named TCR gene transfer-induced graft-versus-host disease (TI-GVHD). In their study, mice treated with TCR-transduced T cells followed by an IL-2 regimen experienced severe autoimmune reaction and had a close to 100% mortality within days after treatment. Further investigations demonstrated that this was also true for T cells which were only transduced with either TCRα or TCRβ alone (Bendle et al. 2010). As TCR surface expression is tightly controlled within T cells and dependent on correct TCR-CD3 subunit assembly, a single TCRα or TCRβ will be retained within cells (Bonifacino et al. 1989). This in turn means that a TCR-mediated autoimmune reaction in the setting of single-chain transfer can only be explained by a heterodimerization of endogenous and introduced chain. The said publication also showed, that when using a modified TCR with somewhat better pairing properties, toxicity could be reduced.

In addition, the expression level of an introduced TCR is reduced by mispairing with an endogenous TCR and heterodimers competing for CD3 assembly. Yet the expression level of a TCR is crucial for T cell function (Labrecque et al. 2001). So, next to potential danger of autoimmunity, mispairing may also limit effectiveness of TCR gene transfer.

Several attempts have been made to tackle this problem. Some approaches aim at limiting heterodimerization by preferential pairing via additional disulfide bonds (Cohen et al. 2007, Kuball et al. 2007) or partial murinization (Cohen et al. 2006). Others diverge more strongly from the natural TCR structure by creating fused TCR-CD3ζ proteins (Willemsen et al. 2000) or single chain TCR (Figure 2) (Bendle et al. 2009). All of these modifications showed less mispairing, however only the single chain and the TCR-CD3ζ approach abolish mispairing completely (Zhang et al. 2004, Sebestyen et al. 2008). In turn, with more structural differences to a native TCR, there is a possible decrease in sensitivity (Zhang et al. 2004) and higher potential for immunogenicity (Uckert et al. 2009).

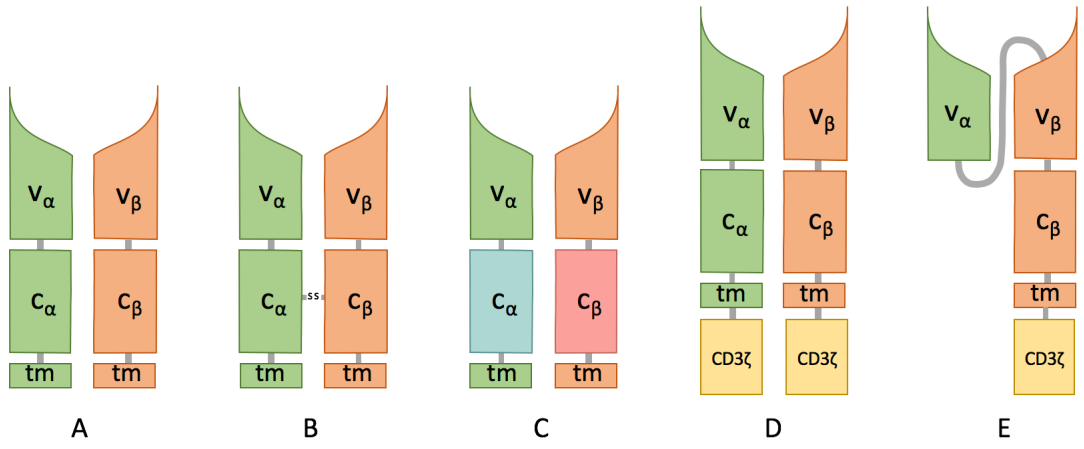

Figure 2: Possible modifications of a native TCR to reduce or avoid mispairing. (A) Native TCR. (B) Additional disulfide bond. (C) Murinization of constant domains. (D) TCR-CD3ζ fusion protein. (E) Single chain TCR (Govers et al. 2010).

3.3 Crossed monoclonal antibodies

Another - albeit less severe - case of mispairing exists in biotechnology: When producing unmodified bispecific antibodies by hybridoma cell lines (so called ‘quadromas’) two heavy and two light chains are produced. The formation of the desired bispecific antibody depends solely on correct pairing. Without further optimization, the yield of the desired antibody is only one tenth of all produced immunoglobulin (Milstein et al. 1983) (Figure 3).

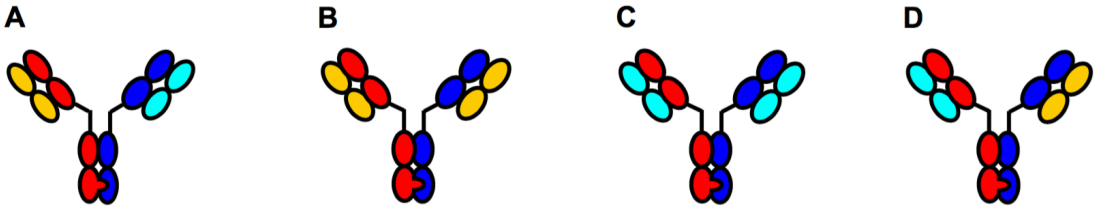

Figure 3: Four of the twelve possible products when producing a desired (A) bispecific antibody. The three undesired side products (B-D) result from mispairing of light chains. The other side products (not shown) result from homodimerization of two identical heavy chains (Schaefer et al. 2011).

Schaefer et al. showed that the possible mispairing between heavy and light chains can be completely abolished by a crossover of either the variable or the constant domains in one antibody arm. The function of such a “CrossMab” is not impaired compared to the unmodified antibody (Schaefer et al. 2011). Schaefer et al. hypothesized that chain alignment works by specific steric interactions of the different domains to their partner domain. That is, a domain of a heavy chain can only pair with the corresponding domain of a light chain. Therefore, a crossover of domains prevents a pairing of a crossed and an uncrossed chain (Figure 4).

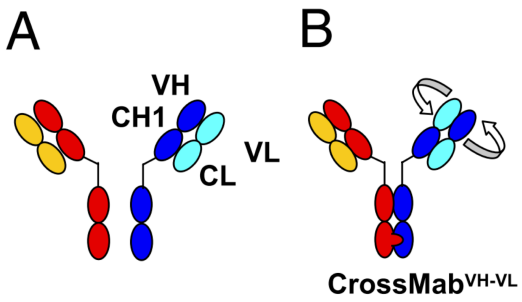

Figure 4: Domain crossover abolishes mispairing of heavy and light chains in bispecific antibodies. Crossing domains of heavy and light chains among each other (B) prevents unwanted heterodimerization of heavy and light chains (i.e. yellow-blue and turquoise-red), which occurs in unmodified antibodies (A) (Schaefer et al. 2011).

3.4 Rationale and goals

Since TCR chains and light chains of antibodies both belong to the immunoglobulin superfamily (Barclay 2003), the approach described above may well translate to mispairing of TCR. In order to evaluate this hypothesis, we designed two “CrossTCR” (xTCR) and assessed their pairing properties and functionality.

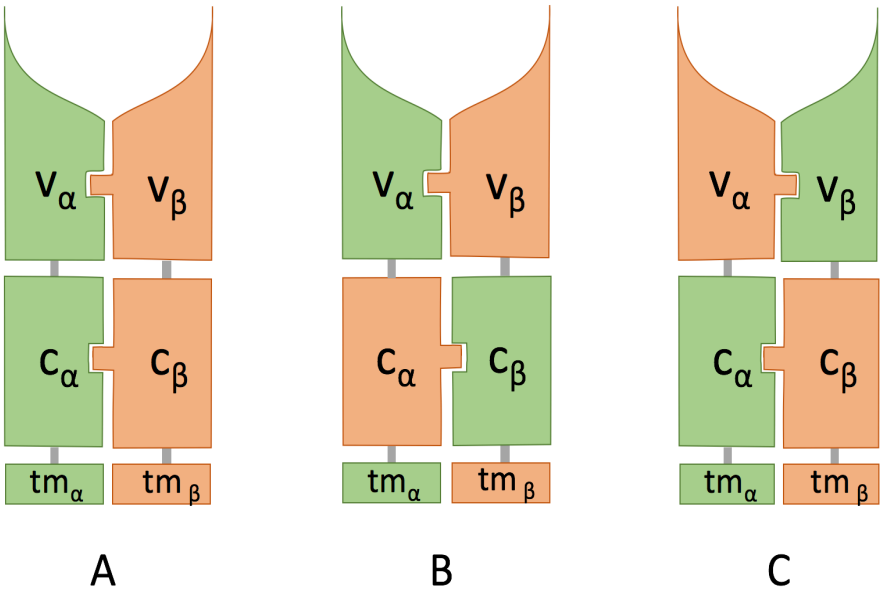

Figure 5: xTCR: By exchanging either the constant (B) or the variable domain (C) of an unmodified TCR (A) two xTCR were designed, to examine their pairing properties and functionality the specific steric interactions between the domains (displayed as ‘knob in hole’) should prevent mispairing of crossed and uncrossed chains.

As a model, we chose the MHC class I-restricted, ovalbumin-specific TCR (OT-I TCR). We considered this the optimal candidate for several reasons: The OT-I model is one of the most common models for testing ACT in mice. There are cancer cell lines such as the Panc-OVA that specifically overexpress the recognized OVA peptide, creating an ideal testing ground for ACT in a mouse tumor model (Kobold et al. 2015). Furthermore, the OT-I TCR showed severe TI-GVHD in the work Bendle et al., supplying an *in vivo* model to test for mispairing side effects. And finally, this approach also allowed for a direct analysis of chain expression via flow cytometry, as there are commercially available antibodies that detect the OT-I TCR α- (i.e. anti-Vα2) and TCRβ-chain (i.e. anti-Vβ5) (de Witte et al. 2008).

In this thesis, the following questions will be addressed:

1. Can crossed T cell receptors be stably transduced into primary murine T cells?
2. Do transduced T cells show surface expression of xTCR?
3. How does the location of domain crossing affect surface expression?
4. Do additional disulfide bonds change xTCR surface expression?

4 Materials

4.1 Chemicals

Table 1: List of chemicals

Acetic acid	Merck, Darmstadt
Agarose	Biozym Scientific, Oldendorf
Calcium chloride	Merck, Darmstadt
Chloroquine	Merck, Darmstadt
Dimethyl sulfoxide (DMSO)	Sigma, Steinheim
Disodium hydrogen phosphate monohydrate	Merck, Darmstadt
Glycerol	Carl Roth GmbH, Karslruhe
Isoflurane	Abbott, Zug
Magnesium chloride	Carl Roth GmbH, Karslruhe
Potassium acetate	Carl Roth GmbH, Karslruhe
Potassium chloride	Merck, Darmstadt
Rubidium chloride	Carl Roth GmbH, Karslruhe
Sodium chloride	Carl Roth GmbH, Karslruhe
Trypan blue	Sigma, Steinheim

4.2 Antibodies

Table 2: List of antibodies

Antibody	Stock concentration	Manufacturer	Clone
Anti-Mouse CD3ε	1.0 mg/ml	eBioscience	145-2C11
Anti-Mouse CD28	1.0 mg/ml	eBioscience	37.51
FITC Rat Anti-Mouse Vα2 TCR	0.5 mg/ml	BD Pharmingen	B20.1
PE Mouse Anti-Mouse Vβ 5.1, 5.2 TCR	0.2 mg/ml	BD Pharmingen	MR9-4

4.3 DNA Primers

Table 3: List of Primers

pMP71 seq fwd	5’-CAG CAT CGT TCT GTG TTG-3’
pMP71 seq rev	5’-CAT TTA AAT GTA TAC CCA AAT CCA-3’
OT-I seq centre	5’-CTG GTC CAA CCA GAC CAG CTT CAC ATG CC-3’
OT-I co seq centre	5’-AGC AAC TAC AGC TAC TGC CTG AG-3’
OT-Iα NotI fwd	5’-ATT AGC GGC CGC GCC ACC ATG GAC AAG ATC CTG-3’
OT-Iα p2A rev	5’-CAA AGT CTG TTT CAC CGG GCT GCT CCA CAG CCT CAG-3’
p2A OT-Iα fwd	5’-CTG AGG CTG TGG AGC AGC CCG GTG AAA CAG ACT TTG-3’
p2A OT-Iβ rev	5’-AGC ACC CGC GGG GCC ATT GGG TTG GAC TCC ACG T-3’
OT-Iβ p2A fwd	5’-ACG TGG AGT CCA ACC CAA TGG CCC CGC GGG TGC T-3’
OT-Iβ EcoRI rev	5’-TAA TGA ATT CTC AGC TGT TCT TCT TCT TCA CCA-3’
OT-Iβ NotI fwd	5’-ATT AGC GGC CGC GCC ACC ATG GCC CCG CG-3’
OT-Iβ p2A rev	5’-GCT GCC GCT GCT GTT CTT CTT CTT CAC CA-3’
p2A OT-Iβ fwd	5’-AAG AAG AAC AGC AGC GGC AGC GGC GC-3’
p2A OT-Iα rev	5’-ATC TTG TCC ATG GGC CCA GGG TTT TCC TC-3’
OT-Iα p2A fwd	5’-CCC TGG GCC CAT GGA CAA GAT CCT GAC CG-3’
OT-Iα EcoRI rev	5’-TAA TGA ATT CTC AGC TGC TCC ACA GCC-3’
scOT-Iα co Not-I fwd	5’-ATT AGC GGC CGC GCC ACC ATG GAT AAG ATC CTG ACC GCC-3’
scOT-Iα c/v EcoRI rev	5’-TAA TGA ATT CTC AGC TGG ACC ACA GCC GC-3’
scOT-Iα va Not-I fwd	5’-ATT AGC GGC CGC GCC ACC ATG GCT CCT AGG GTG CTG G-3’
scOT-Iβ co NotI fwd	5’-ATT AGC GGC CGC GCC ACC ATG GCC CCT AGG GTG-3’

scOT-Iβ va NotI fwd	5’-ATT AGC GGC CGC GCC ACC ATG GAC AAG ATC CTG ACC GC-3’
Signal-β myc-tag rev	5’-CCT CCT CGC TGA TCA ACT TCT GCT CGG TGA CCC AGC TCA GCA G-3’
v-β myc-tag fwd	5’-AGA AGT TGA TCA GCG AGG AGG ACT TGG TGT TTC TGC TGG GCA CC-3’
OTIβ c/v p2A rev	5’-TGC CGC TGC TGT TCT TCT TCT TGA CCA TG-3’
p2A OT-Iα co rev	5’-CTT ATC CAT GGG CCC AGG GTT TTC CT-3’
p2A OT-Iα va rev	5’-GGA GCC ATG GGC CCA GGG TTT TCC-3’
OT-Iα co p2A fwd	5’-CCT GGG CCC ATG GAT AAG ATC CTG ACC GC-3’
OT-Iα va p2A fwd	5’-TGG GCC CAT GGC TCC TAG GGT GCT GG-3’
OT-I ba c/v F131 fwd	5'-AGC AGT ATT GTG GCC CTG GCA CGC G-3'
OT-I ba c/v F131 rev	5'-CCA GGG CCA CAA TAC TGC TCG TAG TTG GCC CG-3'
OT-I ba va Y148 fwd	5'-CGC CGT GTG CCA GCT GAA GGA CCC CAG AA-3'
OT-I ba c/v S157 rev	5'-CGG CCT TGC AAG GCT CGA ACA GGG ACA C-3'
OT-I ba c/v G71 fwd	5'-CGG CGA GTG TCC TGC CCT GCT GAT CTC CAT C-3'
OT-I ba c/v G71 rev	5'-GGG CAG GAC ACT CGC CGG GGA ACT GCT-3'
OT-I ba va Y186 rev	5'-CCA GCA CGC ACT TGT CGG TGA TGA AGG TGC-3'
OT-I ba c/v S197 fwd	5'-CGG CGT GTG CAC CGA TCC CCA GGC CT-3'
OT-I ba c/v S197 rev	5'-GAT CGG TGC ACA CGC CGC TGT GCA CC-3'
OT-I ba co Y148 fwd	5'-CGC CGT GTG CCA GCT GAA GGA CCC TAG-3'
OT-I ba co Y186 fwd	5'-CCG ATA AGT GCG TGC TGG ACA TGA AGG CCA-3'

4.4 Enzymes

Table 4: List of Enzymes

Pfu DNA polymerase	Thermo Scientific
NotI	Thermo Scientific
EcoRI	Thermo Scientific
T4 DNA ligase	Thermo Scientific
Taq DNA polymerase	Thermo Scientific

4.5 Commercial kits

Table 5: List of commercial kits

JetQuick® Gel Extraction Spin Kit	Genomed, Löhne
GeneJET Plasmid Miniprep Kit	Thermo Scientific
PureYield™ Plasmid Maxiprep System	Promega
Plasmid Maxi Kit	QIAGEN

4.6 Buffers

Table 6: List of buffers

Phosphate buffered saline (PBS)	PAA, Paschin
4-(2-hydroxyethyl)-1-piperazineethanesulfonic acid (HEPES)	Sigma, Steinheim

4.7 Media and cell culture supplements

4.7.1 Ingredients

Table 7: List of cell culture media and other additives

Dulbecco's modified Eagles Medium (DMEM)	PAA, Pasching
Roswell Park Memorial Institute 1640 Medium (RPMI)	PAA, Pasching
Penicillin/Streptomycin (100x)	PAA, Pasching
L-Glutamine 200mM	PAA, Pasching
Fetal bovine serum (FBS)	Invitrogen, Auckland
Sodium pyruvate	Biochrom AG, Berlin
G 418 disulfate salt	Sigma, Steinheim
Puromycin	Sigma, Steinheim
Blasticidin	Sigma, Steinheim
β-mercaptoethanol	Sigma, Steinheim
RetroNectin®	Clontech, Mountain View

4.7.2 Prepared media mixtures

Table 8: List of cell culture mixtures

Complete DMEM	DMEM +10% FBS +1% L-glutamine +1% Penicillin/streptomycin
Complete RPMI 1640	RPMI 1640 +10% FBS +1% L-glutamine +1% Penicillin/streptomycin
Plat-E medium	Complete DMEM +10 µg/ml blasticidin +1 mg/ml puromycin
Plat-E hunger medium	DMEM +3% FBS +1% L-Glutamine +1% Penicillin/streptomycin
T cell medium	Complete RPMI +1% Sodium pyruvate +0.1% HEPES buffer
OVA selection medium	Complete DMEM +1 mg/ml G 418

4.8 Cell lines

4.8.1 Platinum E

The Plat-E cell line is based on the traditionally used 293T cell line and is used as a packaging cell line to produce ecotropic retrovirus to transduce murine cells (Morita et al. 2000). Plat-E cells were kept in Plat-E medium described above. Plat-E cells were kindly provided by Matthias Leisegang, Berlin, Germany.

4.9 Devices

Table 9: List of technical devices

Flow cytometer	FACS Canto II (BD)
PCR thermocycler	T3 Thermocycler (Biometra)
Photometer	NanoPhotometer® (IMPLEN)
CO_2 incubator	BD6220 (Heraeus)
Laminar flow cabinet	Lamin Air (Heraeus)
Neubauer chamber	Optik Labor Frischknecht

4.10 Computer Software

Table 10: List of computer software

Flow cytometry analysis	FlowJo (Treestar)
Molecular cloning	Lasergene Suite (DNA star)
Sequencing results evaluation	Lasergene Suite (DNA star)
DNA melting temperature calculation	http://www.appliedbiosystems.com/support/techtools/calc/

5 Methods

5.1 Production of competent DH5α *E. coli*

Bacteria were expanded in 100 ml lysogeny broth (LB) at 37°C to an optical density of 0.40 - 0.55. The medium was then cooled down to 4°C and bacteria were pelleted by centrifugation at 4°C. Supernatant was removed and the bacteria were resuspended in 30 ml of transformation buffer 1. After 5 minutes of incubation at 4°C, bacteria were pelleted once more by centrifugation at 4°C. Finally, the pellet was resuspended in 4 ml transformation buffer 2 and aliquots of 50 – 100 µl were frozen in a liquid nitrogen bath. Hereafter, aliquots were stored at -80°C.

5.2 Primer design

All PCR primers were designed using the DNASTAR Lasergene software suite. When calculating the melting temperature of primers only the annealing part of the primer was considered. Calculation was performed using the tm calculator on www.appliedbiosystems.com/support/techtools/calc. The target annealing temperature for every primer was between 60°C and 65°C.

If, in addition to amplification, an extension by a certain nucleotide sequence was required, primers were designed, comprising two functionally different parts: A 3’ end, annealing to the DNA template, and a 5’ end, consisting of the intended extension sequence.

5.3 Polymerase chain reaction for molecular cloning

In all Polymerase chain reactions (PCR) performed for molecular cloning purposes, only DNA polymerases with proofreading activity were used. The reaction mix was set up in the following way:

Table 11: PCR reaction mix

Component	Amount
Template DNA	50-500 ng
10x Pfu Buffer + $MgSO_4$	5 µl
Primers	50 pmol each
dNTPs	10 nmol each
Pfu DNA polymerase	2.5 U
H_2O	Filled up to 50 µl

The temperature cycling parameters were:

Table 12: PCR cycling parameters

Temperature (step)	Duration	
95°C (initial denaturation)	5 min	
95°C (denaturation)	0.5 min	30 - 35 cycles
Tm – 5°C (annealing)	0.5 min	
72°C (elongation)	2 min/kb	
72°C (final elongation)	10 min	

Next to a simple amplification of the desired DNA fragment, the PCR was also used to add short oligonucleotide sequences to the desired fragment. This was achieved by using the primer design described in 5.2.

Furthermore, PCRs were also utilized to link distinct PCR products together by the so-called overlap extension technique. For this method two sequential PCRs are performed: In a first PCR, each of the desired fragments is not only amplified, but also extended by a matching sequence. This creates an overlap between the two products.

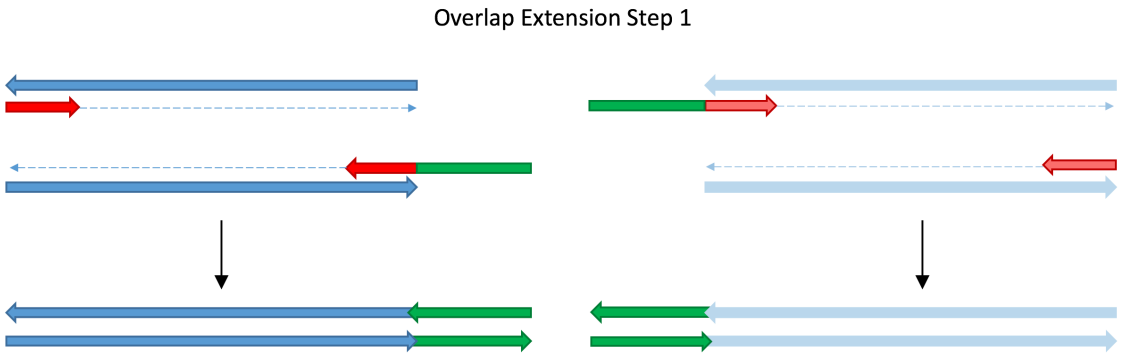

Figure 6: Step 1 of overlap extension PCR: The two inside primers contain a not annealing part (green) by which the two templates (blue) get extended.

In the second PCR, the two products are combined with the two outside primers. Next to an amplification of the template strands, this PCR also yields a DNA fragment, which consists of the two templates linked to each other, because of their ability to also prime each other.

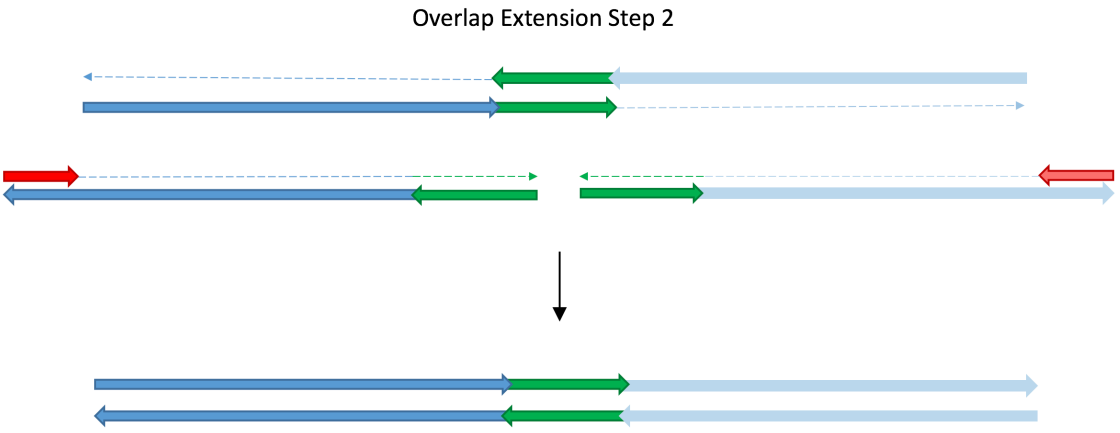

Figure 7: Step 2 of overlap extension PCR: In the second step, only the two outer primers (red) from step 1 are used. On the inside the extensions (green) from step one anneal and function as primers. This step yields a fusion of the two initial templates.

After every PCR, an agarose gel electrophoresis was performed and the correct band was excised and purified using the JetQuick® Gel Extraction Spin Kit according to the manufacturer's protocol.

5.4 DNA agarose gel electrophoresis

For agarose gels, 1.2 - 3.0 g of agarose were dissolved in 150 ml tris-acetic acid-EDTA (TAE) buffer, heated to boiling point and poured into a plastic chamber. Ethidium bromide (0.5 µg/ml) was added and evenly distributed among the liquid. After adding the adequate amount of loading dye, samples were filled into the gel pockets and separated at 90 - 100 V. Fragment size was determined by comparison to a DNA ladder on the gel.

5.5 Sticky end ligation

In order to perform sticky end ligation, insert DNA and vector backbone were first digested with two restriction endonucleases. Any digestion with restriction enzymes was performed according to manufacturer's recommendation, found on www.thermoscientificbio.com/webtools/doubledigest. Digestion time was varied between one and four hours. The reaction mix was incubated at 37°C and was composed as follows:

Table 13: DNA digestion reaction mix

Component	Amount
DNA	500 - 1500 ng
Recommended 10x buffer	2 µl
Restriction enzymes	10 U each
H_2O	Filled up to 20 µl

Digested vector backbone was always purified via agarose gel electrophoresis to clear out the excised former insert. Digested PCR products were directly purified by using the JetQuick® Gel Extraction Spin Kit together with JetQuick® DNA CleanUp Buffers according to the manufacturer's protocol.

Finally, the following ligation reaction mix was set up:

Table 14: DNA ligation reaction mix

Component	Amount
Vector DNA (digested)	Up to 1 mg
Insert DNA (digested)	Up to 500 µg
10x T4 DNA ligase buffer	2 µl
H_2O	Filled up to 20 µl

After 20 - 30 minutes of incubation at room temperature, 10 µl of the reaction mix were used to transform 100 µl competent DH5α E. coli. Competence was induced by preparing E. coli as described in 5.1 and by a 45 second heat shock at 42°C. After 30 - 60 minutes of pre-incubation in LB, bacteria were centrifuged at 400 G for 5 minutes and finally evenly distributed on LB agar plates containing selection antibiotics.

5.6 Cell culture

Cells were always cultured at 37°C under 5% CO_2 and 95% humidity atmosphere. Cells were kept in sterile disposable tissue culture treated flasks or well plates. All cell culture related work was performed with sterile instruments under a laminar flow hood. Whenever cells were spun down this was done by centrifugation at room temperature and 400 G for 5 minutes. Any exceptions are explicitly denoted.

5.7 Cell counting and viability assessment

Cell concentration was determined by adding a certain volume of a trypan blue solution. Only intact cell membranes prevent the blue dye from crossing into the cytoplasm, resulting in a blue staining of dead cells. The concentration of viable cells can then be assessed by counting in a hemocytometer.

5.8 Splenocyte isolation

For splenocyte isolation a mouse of the desired genotype was euthanized under isoflurane anesthesia. The spleen was then harvested via a flank section, remaining soft tissue was carefully removed without rupturing the capsule. For transport the organ was kept in T cell medium. Hereafter, a splenocyte suspension was generated by meshing the spleen through a 40 µm cell strainer and rinsing the strainer several times with T cell medium. The medium passing the strainer was collected in a 50 ml tube and centrifuged. The resulting pellet was resuspended in erythrocyte lysis buffer and incubated for 90 seconds. The lysis reaction was stopped by adding 35 ml T cell medium. The cells were then spun down again and re-suspended in T cell medium.

5.9 Production of retroviruses

On day before transfection 1 - 1.5 x 10^6 Platinum-E cells (Morita et al. 2000) were plated in a well of a tissue culture treated 6-well plate using 3 ml of complete DMEM. The next day, when cells had reached 70 - 90% confluency, the following plasmid solution was prepared.

Table 15: Plasmid solution

	Amount (absolute)	Concentration
Retroviral vector	18 µg	120 ng/µl
$CaCl_2$	30 µmol	200 mM
Chloroquine	38 nmol	253 µM
Sterile H_2O	Filled up to 150 µl	

While incubating the plasmid solution for five minutes, the medium on the Plat-E cells was removed, carefully replaced by Plat-E hunger medium and the cells were placed back in the incubator. A sterile 13 ml polystyrene tube was then filled with 150 µl of transfection buffer and the plasmid solution was added dropwise while constantly vortexing the tube. The combined solution was

incubated for 30 minutes at room temperature and finally added to a well with Plat-E cells.

Six hours later the medium was exchanged for Plat-E transfection medium. After another 42 hours, the virus containing supernatant was harvested and cleared of cells and cellular debris by passing it through a low protein binding 0.45 µm filter. Hereafter Plat-E cells were supplied with T cell medium. After another 24 hours, more the virus harvest procedure from above was repeated.

Collected virus containing supernatant was directly used for transduction purposes.

5.10 Transduction of primary murine T cells

One day before transduction, freshly isolated splenocytes were plated at a concentration of 2 x 10^6 cells/ml in T cell medium supplemented with 50 µM β-mercaptoethanol, 10 U/ml IL-2, 1 µg/ml activating anti mouse CD3ε and 0.1 µg/ml anti mouse CD28 antibody. Cells were then incubated for 24 hours.

The different media used during the entire procedure selectively expand $CD8^+$ cytotoxic T-lymphocytes, while depriving most other cells of necessary survival signals. This way a highly pure (> 99%) cytotoxic T lymphocyte population is obtained from the initial mix of splenocytes.

The following day a tissue culture treated 24-well plate was coated with 400 µl RetroNectin® per well (stock concentration: 6.25 µg/ml). After 2 hours of incubation at room temperature the RetroNectin was removed and wells were blocked for 30 minutes at 37°C using 500 µl of sterile filtrated 2% BSA solution per well. Hereafter, the BSA containing solution was removed and each well was washed once with 2 ml PBS containing 25 mM HEPES.

Depending on viral titers 1-2 ml harvested virus (or the equivalent of concentrate in T cell medium) was added to each well. The plate was then centrifuged at 4°C, 3000 g for 2 hours to attach viral particles to the RetroNectin layer.

In the meantime, cultivated splenocytes were counted, centrifuged and supplied with fresh T cell medium containing 50 µM β-mercaptoethanol and 10 U/ml IL-2. Cell concentration was adjusted to 1 x 10^6/ml.

When virus centrifugation was completed, remaining medium was removed, and 1 ml of splenocyte containing medium was added to each virus coated well. Additionally, one uncoated well was included as an untransduced control. Finally, 10 µl of mouse T-activator CD3/CD28 Dynabeads® were added to each well and the plate was centrifuged for another 30 minutes at 800 G and 32°C.

After an incubation period of 24 hours, 1 ml of the second virus harvest was added to the matching well and spun down for 90 minutes at 800 G and 32°C. Cells were then placed in the incubator for 6 hours and afterwards 1 ml of medium was carefully removed and exchanged for fresh T cell Medium with 50 µM β-mercaptoethanol and 10 U/ml IL-2.

The following day and every second day hereafter, cells were centrifuged and concentration adapted to 1 x 10^6 cells/ml. From this day onward, cells were cultivated in T cell medium supplemented with 50 µM β-mercaptoethanol and 50 ng/ml IL-15.

Transduction efficiency was determined by flow cytometry between 24 and 72 hours after second transduction.

Transduced or untransduced expanded mouse T cells were never used for experiments later than eight days after splenocyte isolation.

6 Results

6.1 Transduction of primary murine T cells with the OT-I TCR

The unmodified ovalbumin specific T cell receptor, which served as a control throughout all experiments, was first cloned into the pMP71 vector. To achieve a high level of co-expression a bicistronic vector design was implemented. This was done by using a DNA sequence encoding for a p2A peptide.

When T cells were transduced with this vector, the surface expression profile in flow cytometry showed only expression of the β-chain of the OT-I TCR. During further analysis, an intracellular staining of the transduced T cells was performed, revealing that the α-chain was indeed properly transcribed but retained within the cells (Figure 8).

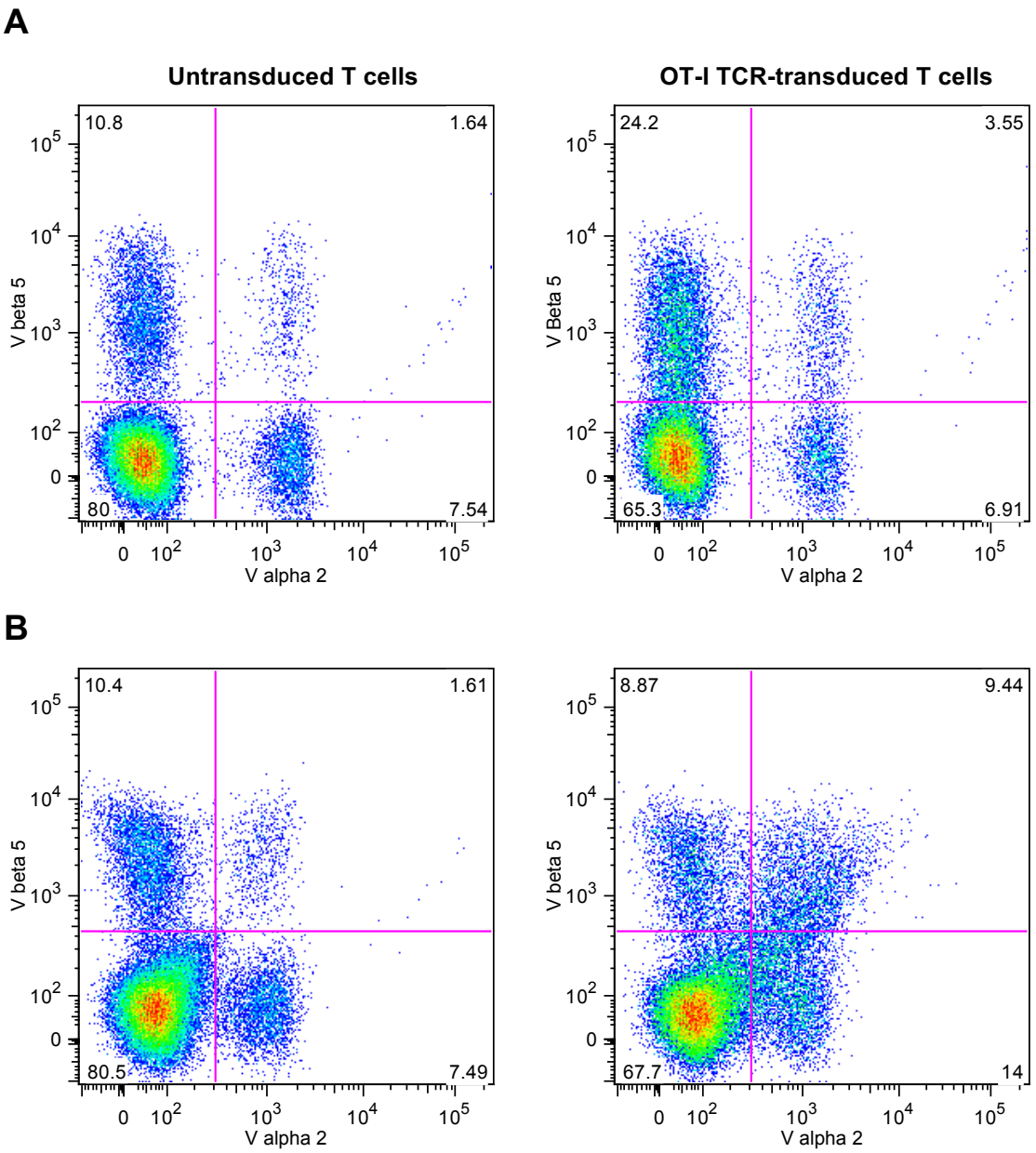

Figure 8: Flow cytometry analysis of transduced T cells. Surface (A) and intracellular (B) staining for vα2 and vβ5 of OT-I TCR-transduced (right) versus untransduced (left) T cells.

To determine whether the order of the chains relative to the p2A linker impacts the expression profile, the chain order within the construct was reversed, so that now the β-chain preceded the p2A sequence.

The reversed order not only led to a correct localization of the α-chain, but also left the localization of the β-chain unaffected (Figure 9). Therefore, this construct was used for all further transductions.

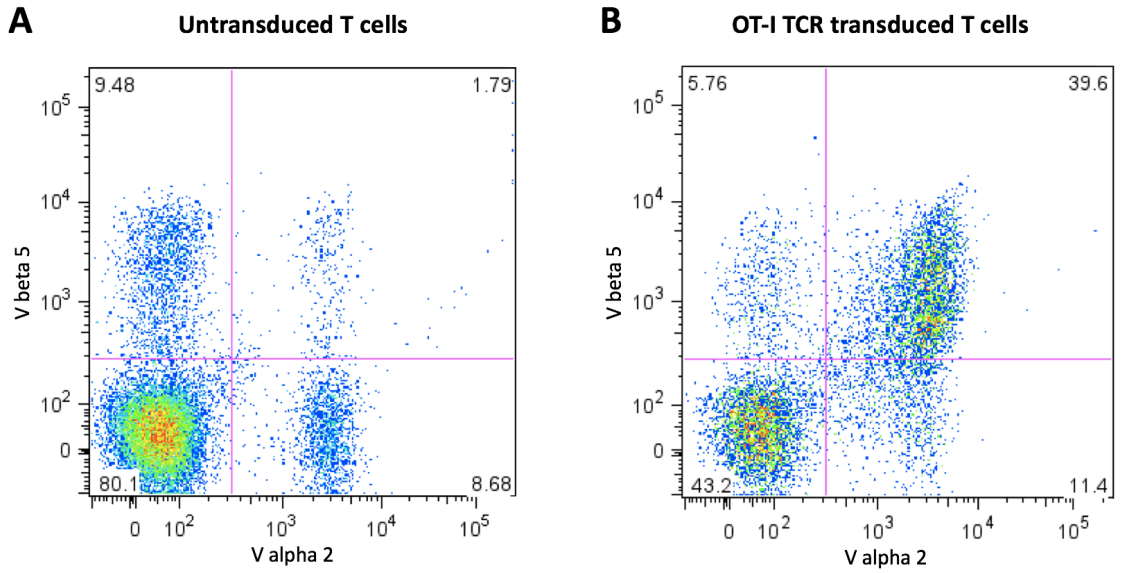

Figure 9: Flow cytometry analysis of transduced T-cells. Surface staining for vα2 of reversed OT-I TCR transduced (B) versus untransduced (A) T cells

6.2 Design of cross T cell receptors

On first approach the following two xTCR were constructed:

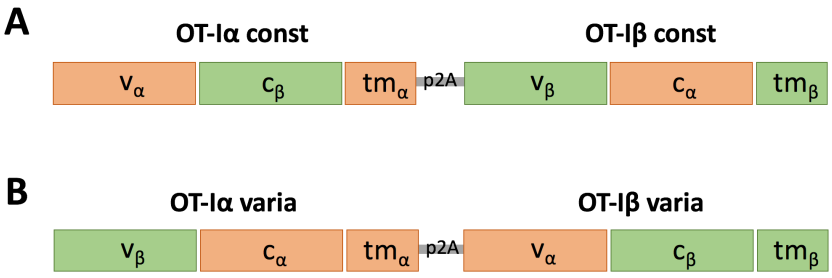

Figure 10: Primary xTCR design: Linearized map of the OT-I const (A) and OT-I varia (B) xTCR within the vector, showing the location of the different domains and order in respect to the linker sequence. Chains are referred to as alpha or beta chains depending on their transmembrane domain.

The two xTCR were named by the domain that was crossed. The one being the (OT-I) const xTCR (Figure 10 A) and the other the (OT-I) varia xTCR (Figure 10 B). When referring to the chain subtype (alpha or beta) we decided to name an xTCR chain according to its transmembrane domain as this domain was never crossed in any of our constructs. That is, a chain carrying the alpha transmembrane domain would be referred to as OT-Iα varia or OT-Iα const depending on xTCR type. The same holds true for a chain carrying the tm beta domain (labelling shown in Figure 10)

6.3 Transduction of cross T cell receptors

After transducing both variants of the xTCR into primary murine T cells, surface profiling in flow cytometry did not reveal any differential surface expression of the xTCR chains (Figure 11 A and Figure 11 B). Due to our previous experiences, we again performed intracellular staining which revealed differential expression only of Vα containing chains (Figure 11 C and Figure 11 D).

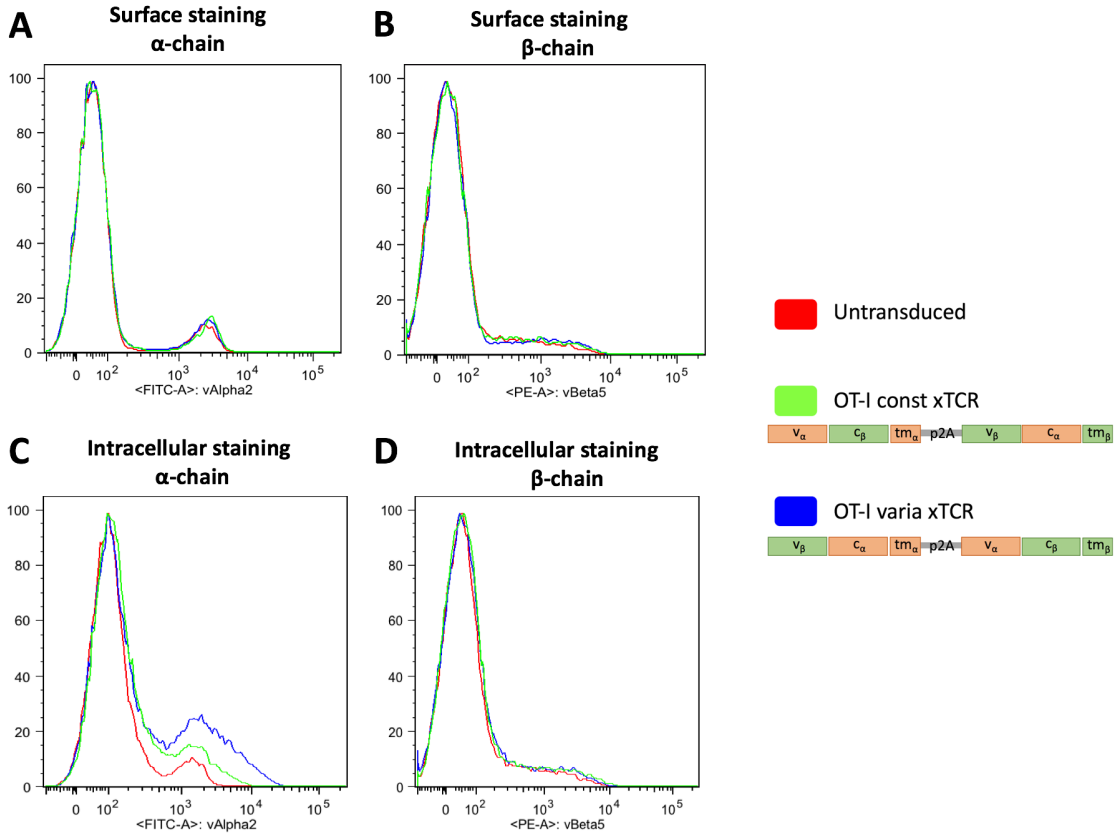

Figure 11: Flow cytometry analysis of xTCR transductions: Staining for vα2 (A, C) and vβ5 (B, D) of untransduced (red), const xTCR (green) and xTCR transduced (blue) T cells. The top half (A, B) shows surface staining, the bottom half intracellular (C, D) staining.

To further investigate this issue, we decide to construct single chain vectors, so we could analyze surface expression independent of possible p2A residue interference.

6.4 Single chain xTCR vectors

The following four chains were cloned into individual vectors, to allow single chain transduction of T cells:

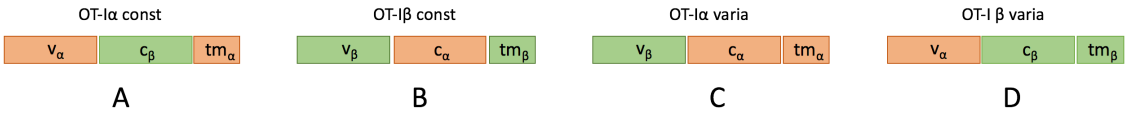

Figure 12: Single chain xTCR constructs: The two chains of each construct were separately cloned into one vector each yielding four new constructs, named according to their transmembrane domain and the crossing type (A-D). The individual chains were left unchanged.

Again, we named the chains ‘const’ (Figure 12 A and Figure 12 B) or ‘varia’ (Figure 12 C and Figure 12 D) depending on the crossing type. A chain was referred to as α-chain (Figure 12 A and Figure 12 C) or β-chain (Figure 12 B and Figure 12 D) by its respective transmembrane domain. After transducing T cells, we then again performed surface and intracellular staining for vβ5 and vα2 followed by flow cytometry analysis.

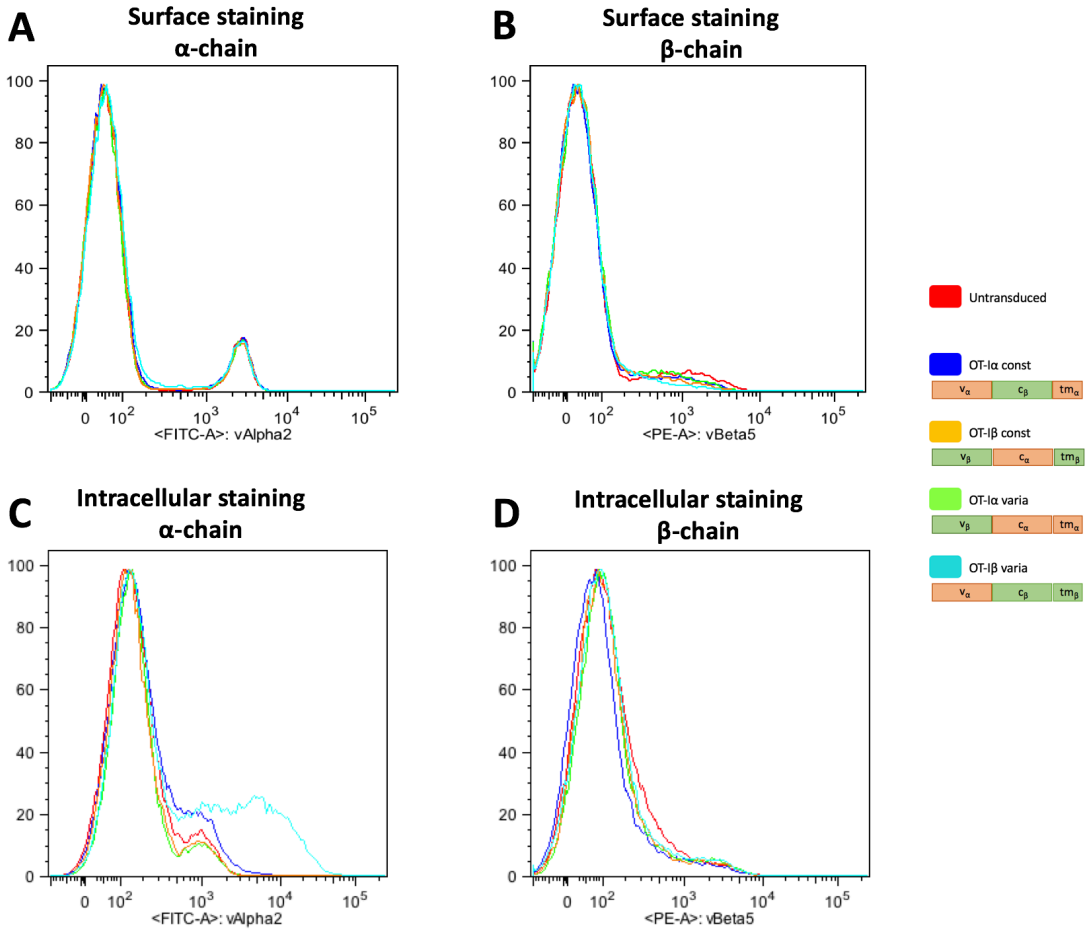

Figure 13: Flow cytometry analysis of single chain xTCR transduction: Vα2 (A, C) and vβ5 (B, D) staining of the different xTCR single chains (color coding far right). The top half (A, B) shows surface staining, the bottom half (C, D) intracellular staining.

None of the single chain constructs expressed on the surface (Figure 13 A and Figure 13 B), yet there was intracellular expression of the chains carrying a variable alpha domain (Figure 13 C). However, there was no detectable expression of any chain when staining for vβ5 (Figure 13 B and Figure 13 D). To further evaluate the impact of the linker sequence we proceeded by changing the order of our xTCR constructs within the vector.

6.5 Reversed xTCR double chain vectors

We reversed the order of our xTCR chains as follows:

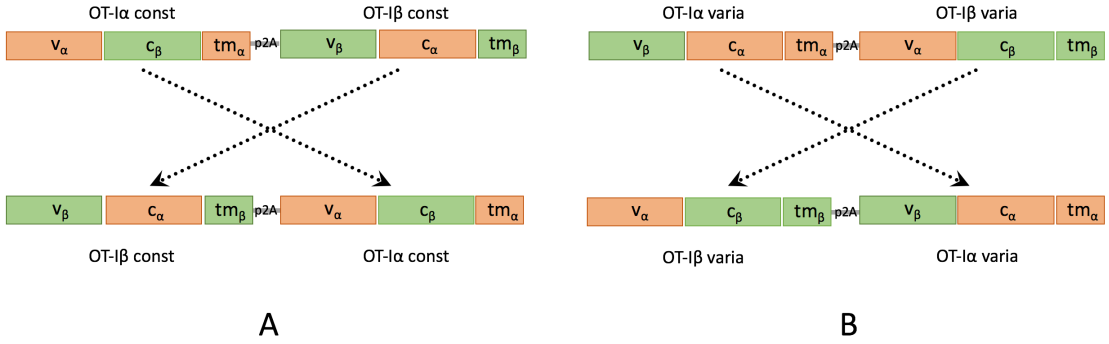

Figure 14: Reversed xTCR vectors: In both the constant (A), as well as the variable (B) domain crossed TCR we reversed, we reversed the order of the chains relative to the linker sequence.

Thereby, the large part of cleaved p2A peptide residue would now be attached to a tm β domain in both constructs (Figure 14 A and Figure 14 B). The following transduction results were obtained:

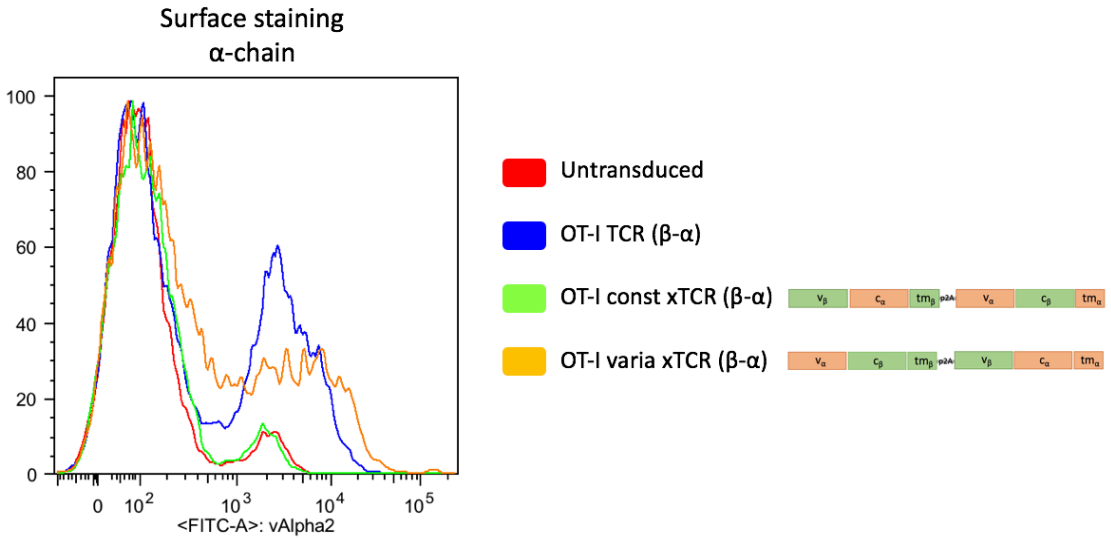

Figure 15: Flow cytometry analysis of reversed xTCR transduction: Surface staining for vα2 of untransduced (red), reversed OT-I (blue), reversed const xTCR (green) and reversed varia xTCR (orange) transduced T cells.

While the transduction efficiency was considerably below our usual transduction efficiency and the transduction efficiency seen in the unmodified TCR there was a clear surface expression of the OT-I varia xTCR. There was still no intra- or extracellular signal of vβ domains (data not shown). However, when further investigating the properties of the OT-I varia xTCR surface expression changed.

6.6 xTCR surface kinetic

Through different experiments we observed that the surface expression of our OT-I varia xTCR was unstable (Figure 16).

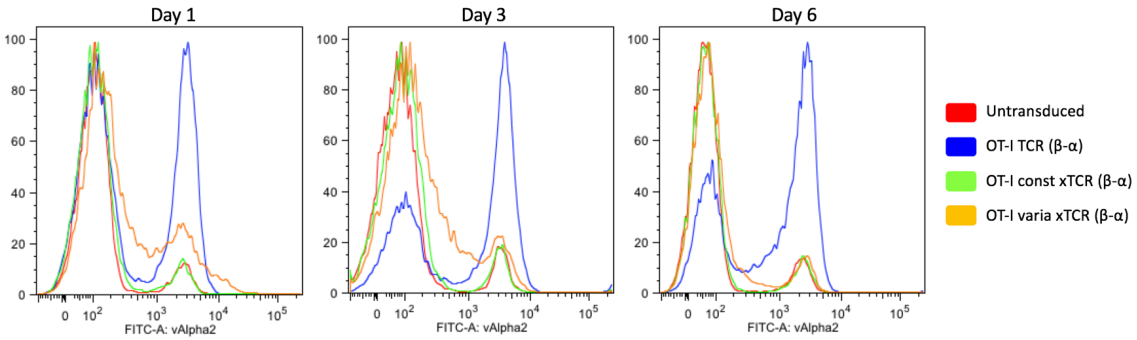

Figure 16: Flow cytometry analysis of xTCR surface expression over time: Surface staining for vα2 on day 1 (left), day 3 (middle) and day 6 (right) after primary transduction of the different constructs (color coding far right).

While on day one there was still a clear – albeit low –expression level, surface expression continuously decreased to baseline over the course of six day. To determine if this was a problem of location or expression on protein level, we performed intracellular staining.

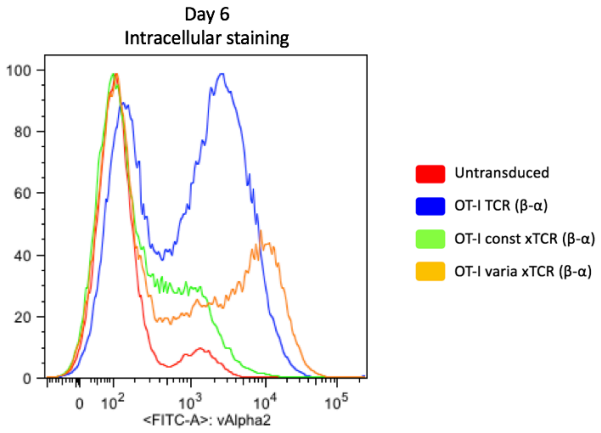

Figure 17 Flow cytometry analysis on day 6 after transduction. Intracellular staining for vα2 of the different constructs (color coding on the right).

Despite no surface expression there was still a relatively high level of OT-I varia xTCR detectable within the cells. Here, also the OT-I const xTCR was expressed, though at a very low level (Figure 17). To further investigate this, we evaluated if surface expression could be enhanced by stronger binding of the xTCR chains.

6.7 Disulfide bond xTCR

We derived this idea from early TCR engineering approaches, in which selective pairing was tried to be achieved by adding a disulfide bond between the two introduced chains. S. Dengl and W. Schaefer (Roche AG, Penzberg) kindly provided the protein structure simulations, identifying three possible domains for insertion of a disulfide bond (Figure 18).

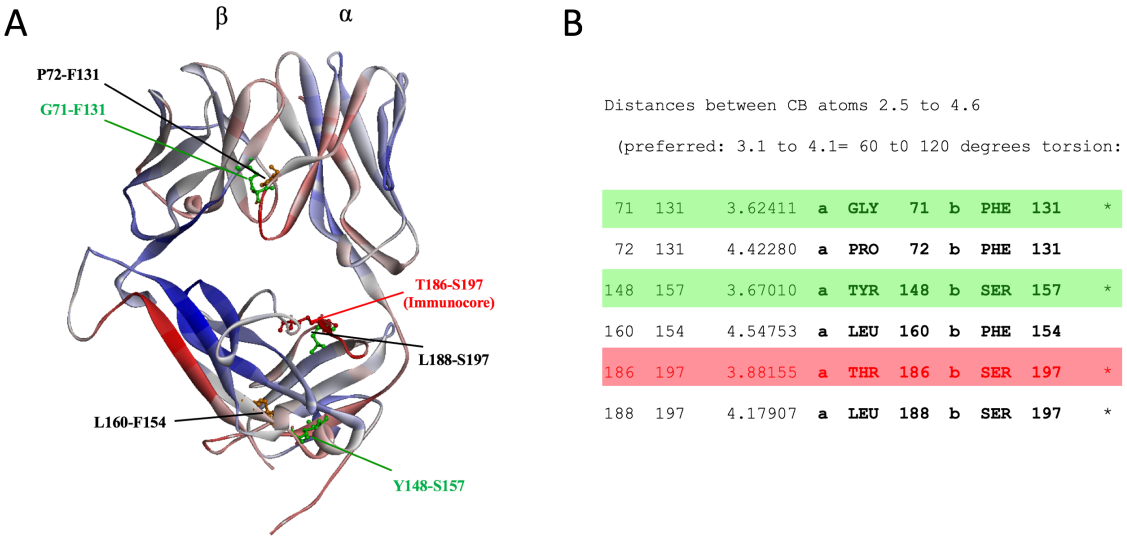

Figure 18: TCR structure simulation: Simulation of the OT-I TCR tertiary structure (A). Six possible sites were analyzed as candidates for disulfide bonds. Their CB atom distance and their degree of torsion was calculated (B). The locations marked with green were chosen as best candidates. The red location is one commonly used as introduction site for disulfide chains and was therefore also realized. Provided by W. Schaefer and S. Dengl, Roche AG, Penzberg

These three candidates were generated, resulting in a total of six new vectors, each now encoding for one of three possible disulfide bonds (Figure 19 A-C).

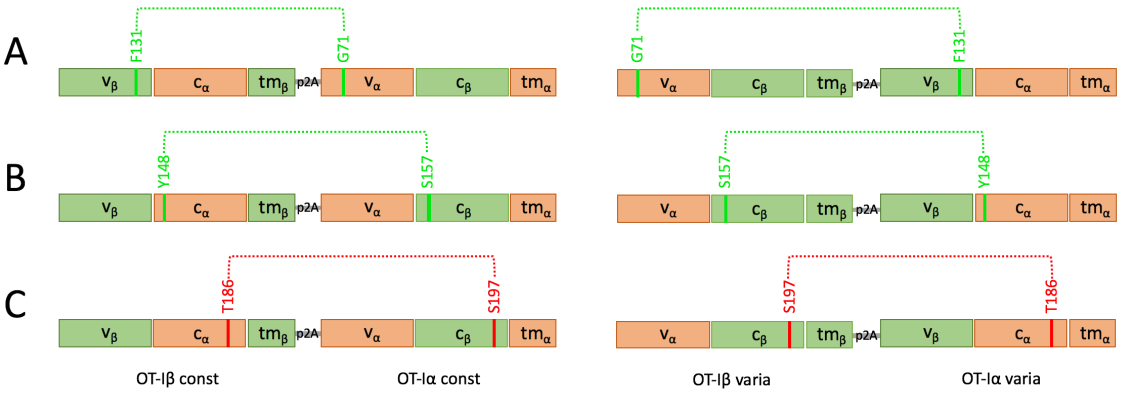

Figure 19: Cysteine residue insertion locations: The two xTCR (left and right) vectors were changed at the marked locations, so that the given amino acids were replaced with cysteine. Thereby introducing the

three calculated disulfide bonds (dotted lines) between the two xTCR chains shown above. The locations shown in A-C correspond to the locations calculated in Figure 18 B.

Again, these constructs were transduced into primary murine T cells to compare their surface expression profile to the respective OT-I xTCR.

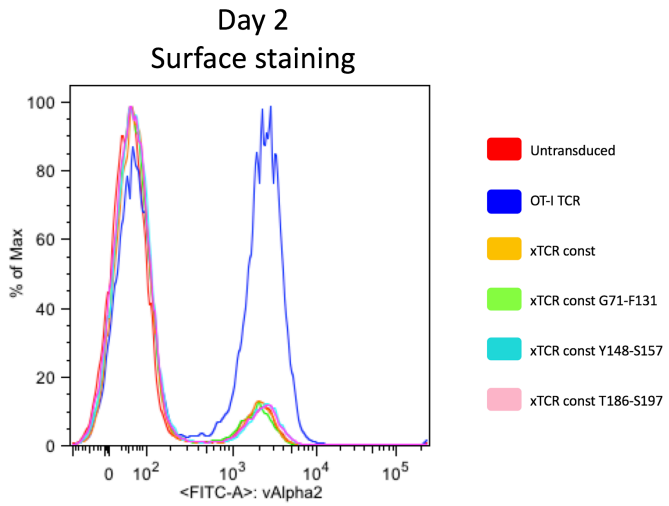

Figure 20: Flow cytometry analysis of disulfide bonds in xTCR const transductions: Surface staining for vα2 on day 2 after primary transduction with the different cysteinized const xTCR vectors (color coding on the right).

In the case of the OT-I const xTCR, there was no detectable surface expression (Figure 20). In the case of the OT-I varia xTCR, there was detectable vα2 surface expression. However, all three cysteine-modified xTCR variants did neither significantly increase surface expression on day two, nor show stable surface expression over time (Figure 21). By day five all transductions displayed baseline surface levels of vα2.

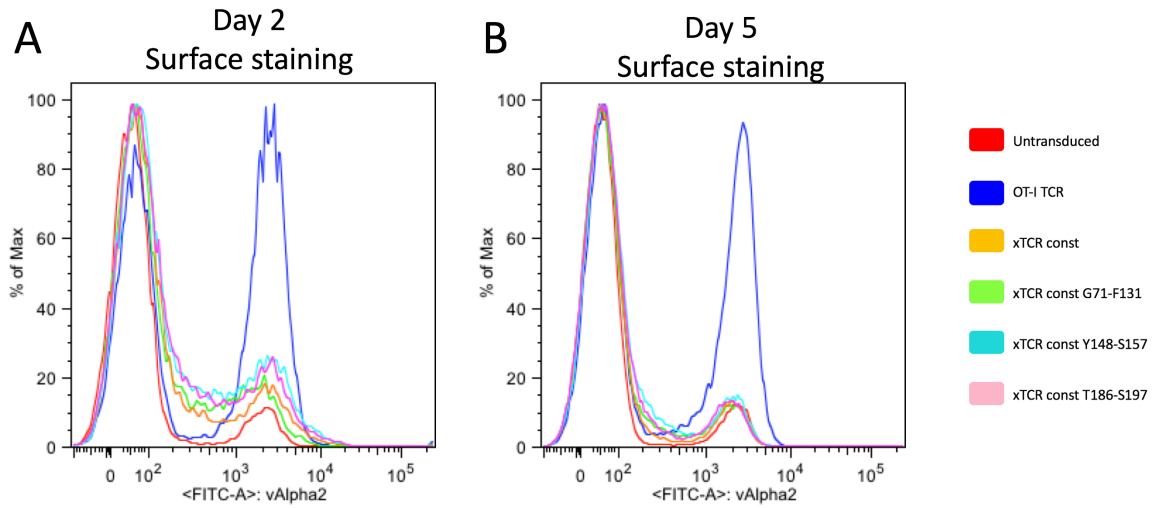

Figure 21 Flow cytometry analysis of disulfide bonds in xTCR varia transductions: Surface staining for vα2 on day 2 (A) and day 5 (B) after primary transduction with the different cysteinized varia xTCR vectors (color coding on the right).

6.8 Elbow regions

In our initial approach, the exact location of the domain switch was chosen within the elbow region, that is the linking sequence between constant and variable domain (Figure 22).

Vα... eqyfgpgtrl**tvl** – **pdiqnpepavy**qlkdp ...Cβ

Vβ... yqliwgsgtkl**iik** – **edlrnvtpp**kvslfepsk ...Cα

Figure 22 Amino acid sequence of domain switch region: The underlined amino acids represent the putative elbow region and the black dash the location of the domain switch. The annotations on the side and the color coding indicates whether the amino acids belong to α- or β-chain.

In an attempt to restore continuous surface expression of the xTCR, we changed the location of the domain switch so that the elbow region was left intact, that is we moved the location of the domain crossing to either edge of the elbow region (Figure 23).

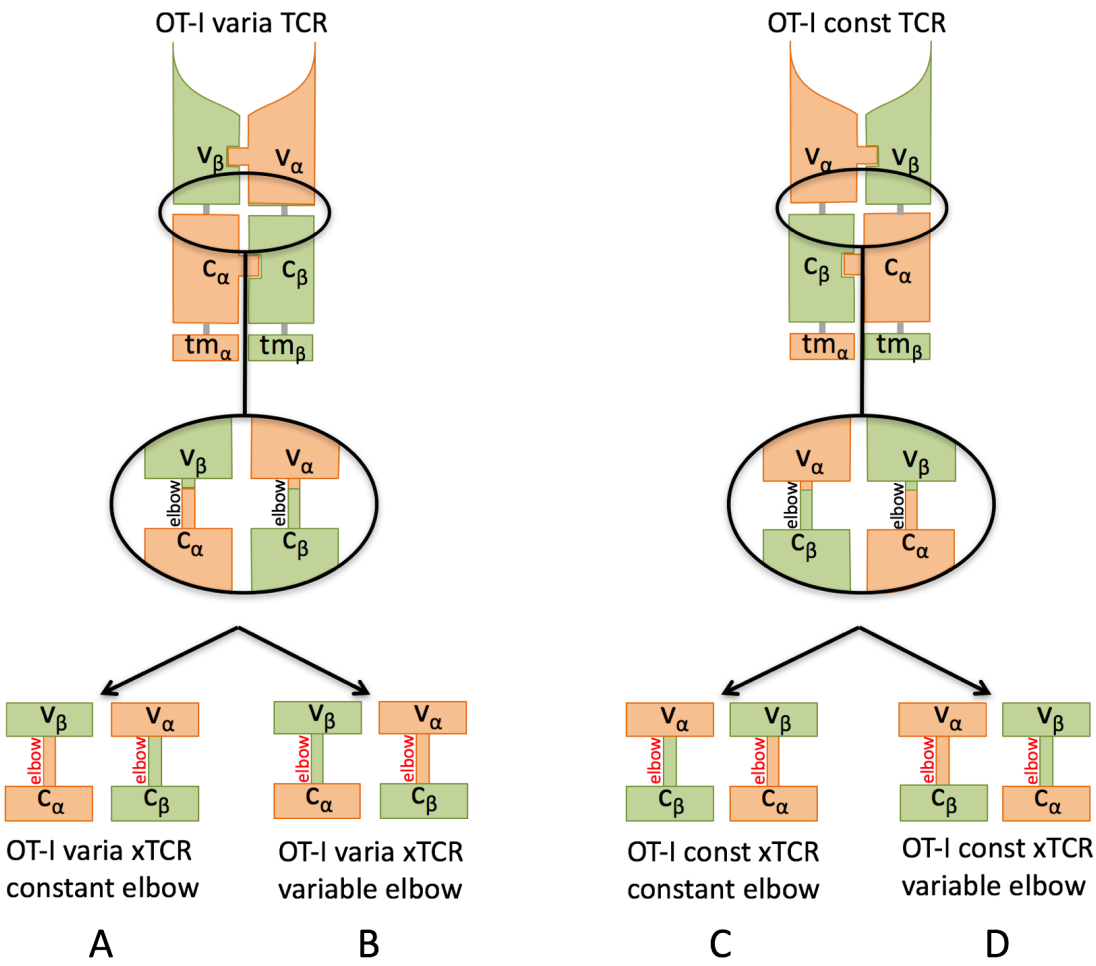

Figure 23: Elbow region remodeling: Of our two initial xTCR (top) in which the elbow was 'cut' centrally we designed a total of four elbow modified xTCR in which the elbow region was left intact, named according to the domain the elbow region belongs to (A-D).

This resulted in a total of four newly designed xTCR constructs, two for each domain crossing type (Figure 23 A and Figure 23 B, Figure 23 C and Figure 23 D respectively). One in which the elbow was left uncrossed (Figure 23 A and Figure 23 D), and one where the elbow was crossed along with the adjacent domain (Figure 23 B and Figure 23 C). Despite several attempts, we were unfortunately not able to successfully clone the OT-I varia TCR with variable elbow (Figure 23 B). So, we decided to proceed with only three constructs. Again, we transduced the xTCR into primary murine T cells and analyzed by flow cytometry.

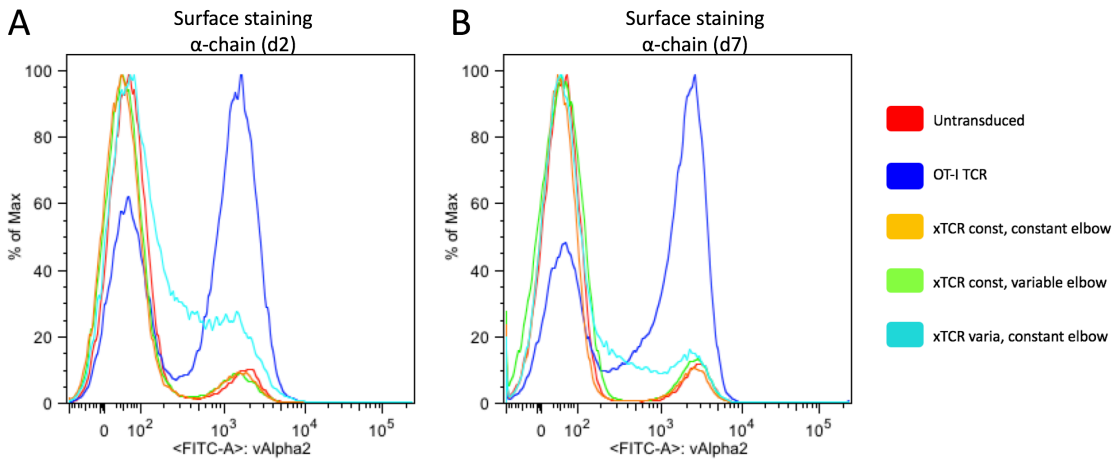

Figure 24: Flow cytometry analysis of transductions of xTCR with modified elbow region: Surface staining for vα2 on day 2 (A) and day 7 (B) after primary transduction of the different elbow modified xTCR vectors (color coding far right).

We observed, that OT-I varia xTCR based modification showed significantly increased surface levels on day two (Figure 24 A). Yet, surface levels declined over time (Figure 24 B). The OT-I const based constructs showed no increased surface expression (Figure 24 A and Figure 24 B). When directly comparing the xTCR varia with and without modified elbow, we saw slightly higher expression levels in the changed elbow construct (Figure 25 A). Still, both transductions showed decreasing surface expression levels over time (Figure 25 B).

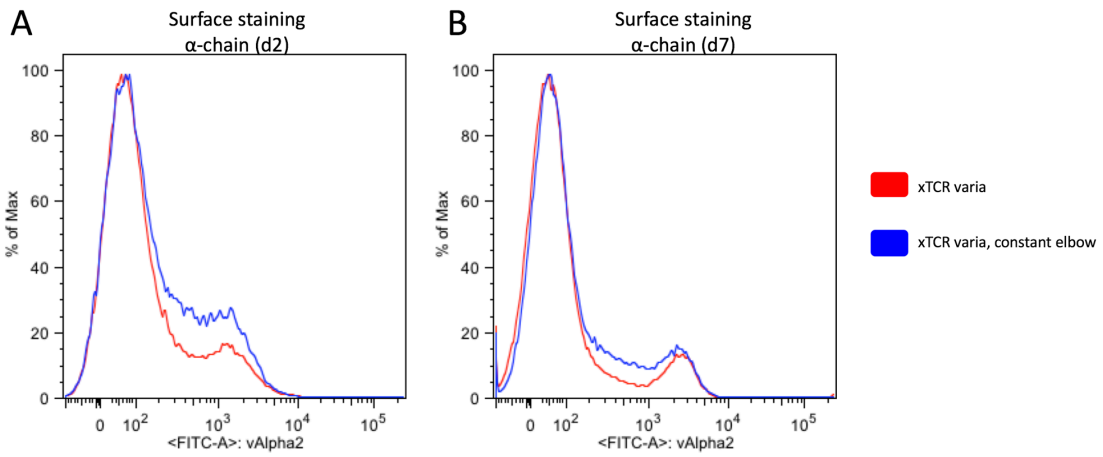

Figure 25: Flow cytometry analysis of varia xTCR and elbow modified varia xTCR: Surface staining for vα2 on day 2 (left) and day 7 (right) after primary transduction with xTCR varia (red) or xTCR varia with modified elbow (blue).

7 Discussion

7.1 Summary

Taken together our experiments show that xTCR can be transduced into primary murine T cells resulting in initial surface expression of at least the β-chain of the OT-I varia xTCR. However, surface expression diminishes over time returning to baseline about seven days after transduction. At the same time, intracellular expression of vα carrying chains of both xTCR variants remains constantly high.

We also observed that when using bicistronic vectors the order of the two inserts is relevant. More precisely, we found that whenever an alpha transmembrane domain was located N-terminally of the p2A linker, the corresponding chain did not translocate to the surface, despite being expressed intracellularly.

Furthermore, surface expression of the OT-I varia xTCR depended on co-transduction of both chains. Single chain transduction did not result in surface expression.

Additional disulfide bonds did not change surface expression profile of xTCR irrespective of their location within the xTCR.

Variation of the crossing point within the elbow region slightly improved surface expression levels. However, decrease of surface expression over time could not be prevented.

7.2 Linker sequence

During all our experiments, we used the linker sequence known as p2A.
2A peptide sequences mediate co-translational self-cleavage, without interfering with translation itself, thus leading to a stoichiometric 1:1 ratio of the two proteins (Szymczak et al. 2005). The cleaved peptide residue remains

linked to the translated proteins (Kim et al. 2011). All bicistronic transductions, in which an alpha transmembrane domain preceded the p2A linker, the N-terminal insert failed to translocate to the surface. When transducing the unmodified OT-I TCR, the β-chain translocates to the surface – irrespective of its relative position to the p2A linker. TCR translocation depends critically on correct assembly of both TCR chains and CD3 subunits (Bonifacino et al. 1989, Bonifacino et al. 1990). The assembly of CD3 subunits with the TCR mainly depends mainly on charged residues in the transmembrane domain of the TCR and CD3 chains (Call et al. 2002). A tm α domain that is not paired to CD3 subunits is subjected to rapid intracellular degradation (Bonifacino et al. 1990). Therefore, the most plausible hypothesis that explains our observations seems to be, that the 19-aminoacid residue of p2A sequence interferes with a correct TCR-CD3 complex assembly. Due to its location, it seems most likely that the disruption occurs mainly between the TCRα and the CD3 subunits. Interestingly, this does not seem to be the case for the TCRβ.

However, literature shows that p2A interference does not occur consistently in every TCR (Leisegang et al. 2008). It can therefore not be taken for granted that p2A residues never interfere with TCRβ-CD3 assembly. Even if surface expression of a TCR chain is not completely abrogated, it is possible for p2A residues to impair CD3 assembly. This can result in the native TCR outcompeting the exogenous TCR for CD3 recruitment and lowering its density on the surface, thus decreasing functional activity (Heemskerk et al. 2007, Jorritsma et al. 2007).

Alternative strategies to avoid usage of p2A linkers include using internal ribosome entry sites (IRES) or performing double transductions with monocistronic vectors. However, both approaches suffer from drawbacks, as they cannot achieve a 1:1 stoichiometric ratio of both TCR chains, which in turn leads to suboptimal surface expression. Especially double transductions suffer from low transduction efficiency, while IRES linked vectors tend to underexpress the C-terminal insert (Leisegang et al. 2008). Therefore, while alternatives to p2A linkage are desirable, current substitutes are considered

inferior. Until better options arise, p2A linked bicistronic TCR vectors need to be assessed carefully on a case by case basis.

7.3 Vβ5 epitope loss

Throughout all our experiments and despite several modifications to the initial xTCR approach we were never able to detect the vβ5 epitope once the domains were switched. We considered several possible explanations. Two of which we believed to be the most relevant:

For one, it is possible that the tertiary structure of the respective xTCR changes significantly over a larger area including the vβ5 epitope. If a change of the tertiary structure occurs at the epitope it is likely that major parts of the tertiary structure of this chain are affected. As opposed to immunoglobulins especially the β elbow region is considered more rigid (Bentley et al. 1995).

However, if domain crossing affects the overall tertiary structure of one chain, one would expect an impact on the tertiary structure of the second chain. Yet, our results suggest that the structure of this chain is conserved, as the vα2 epitope remains intact. Also, if the tertiary structure were the main issue then it would be likely that this can be reverted by choosing a better site to cross. But in our experiments three different crossing sites within the elbow region showed the same loss of detectability. And finally, immunoglobulins and TCR show high amounts of homology (Boulot et al. 1994) but domain switching has no major impact on the structure of immunoglobulins (Schaefer et al. 2011).

Another explanation is that the vβ5 epitope lies exactly at the elbow region of the TCRβ. Unfortunately, the exact location and sequence of the vβ5 epitope are unknown so we were unable to prove this hypothesis. But given the arguments above, we deem this more likely to be true than a large change of tertiary structure. To be certain, further experiments need to be conducted, to either determine the vβ5 epitope or the crystal structure of xTCR.

7.4 Pairing properties

Despite not being able to detect the vβ5 epitope, we were still able to draw conclusions about the pairing properties of our xTCR constructs. These became especially apparent when looking at our single chain transduction results:

Through intracellular staining we could prove that at least the transduction of OT-Iα const and OT-Iβ varia was successful. However, there was no detectable surface expression. If these chains mispaired with endogenous TCR chains to form functional TCR-CD3 complexes, then these complexes would translocate to the surface (Bonifacino et al. 1989). As we detected no surface expression in our single chain experiments, we therefore concluded that none of our detectable crossed chains mispair with endogenous TCR chains.

Furthermore, we could show that in our variable domain switch temporary surface expression is re-established, once we transduce with both chains. Together with our single chain data, this strongly indicates that the undetectable OT-Iα varia chain pairs with the detectable OT-Iβ varia chain and allows for correct CD3 subunit assembly, resulting in increased detectable vα2 epitope expression. So, despite one of our chains being undetectable, we can confidently assume that we did in fact achieve surface expression of both chains, as only correctly assembled TCR-CD3 complexes avoid intracellular retention and degradation (Bonifacino et al. 1990). By the same reasoning we can also assume, that the pairing properties of the constant domain switch were not sufficient to allow for a correct TCR-CD3 complex assembly.

7.5 Kinetics of surface expression

We were able to prove that xTCR can be transduced into primary murine T cells by intracellular flow cytometry staining. As p2A linked bicistronic vectors yield a 1:1 stoichiometric ratio of both inserts (Szymczak et al. 2005), intracellular detectability of one chain, guarantees successful translation of both chains.

Our experiments also show that the OT-I varia xTCR is expressed on the surface of transduced T cells. The explanation why surface detectability of one chain proves successful surface expression of both chains was already given in 7.4.

However, surface expression was not permanent, but subject to some mechanism of degradation or internalization, leading to a continuous decrease of surface-detectable vα2 epitope. Eventually, surface expression returns to baseline after about seven days post transduction.

The possibility that the transduction itself is unstable and gene expression is downregulated can be excluded, as there is durable intracellular expression of xTCR. Only surface expression diminishes.

We were unable to find literature describing a continuous decrease of TCR surface expression post transduction. Literature consistently emphasizes that only completely assembled TCR-CD3 complexes translocate to the surface (Klausner et al. 1990). So, deterioration of TCR surface-levels cannot be explained by unsuccessful TCR-CD3 assembly. There are however, mechanisms described in literature that combined could potentially explain our observations:

First, there is a concept of native TCR “outcompeting” an introduced TCR for CD3 recruitment (Bethune et al. 2016). The idea is based on the fact that the CD3 subunit pool is limited. If a second TCR is introduced into a cell, the concentration of TCR in the cell rises, while the number of available CD3 molecules does not. Therefore, TCR dimers compete for CD3 assembly. If the native TCR shows a higher affinity to CD3 subunits, resulting in preferential pairing, then less TCR-CD3 complexes of the introduced TCR will form. In turn, this would lead to less surface translocation of the introduced TCR.

Secondly, TCR-CD3 complexes get internalized and lysosomally degraded when T cells activate (Valitutti et al. 1997). During our transduction protocol, a

highly pure $CD8^+$ T cell population is achieved by various forms of stimulation and activation.

Taking together both of these effects, the following hypothesis seems plausible: xTCR show a lower affinity to CD3 molecules than the native TCR. Initially, however, the availability of intracellular CD3 subunits is high (Figure 26 A). Therefore, a number of xTCR-CD3 complexes form and translocate to the surface (Figure 26 B). Here, both xTCR- and native TCR-CD3 complexes get internalized and degraded due to T cell activation (Figure 26 C). This in turn, “consumes” more CD3 molecules than are produced, lowering the intracellular availability of CD3 subunits. However, the intracellular TCR levels remain high, as the cell produces two types of TCR. Due to the greater imbalance of TCR chains and CD3 subunits, the native TCR now increasingly outcompetes the xTCR for CD3 recruitment (Figure 26 C). This continuously lowers the amount of surface expressed xTCR and results in intracellular accumulation of xTCR (Figure 26 D).

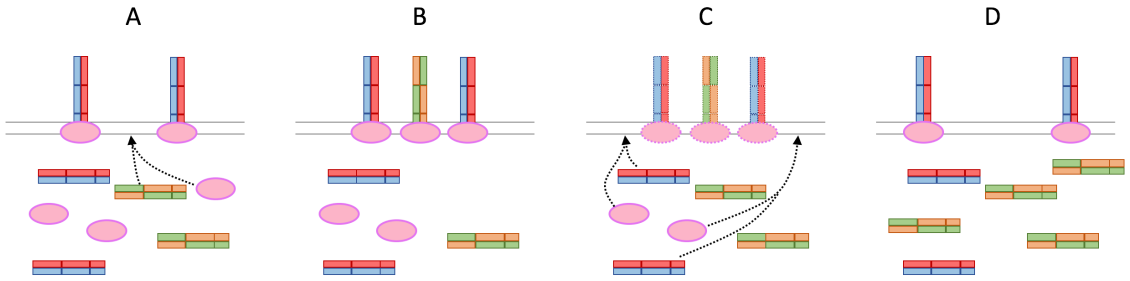

Figure 26: Hypothesis for xTCR surface kinetics: Each subfigure shows a T cell membrane with native (blue/red) TCR and xTCR (green/orange), as well as CD3 molecules (pink, simplified). First, intracellular levels of CD3 are high (A), allowing xTCR surface expression, but lowering CD3 levels (B). Then, surface TCR-CD3 complexes are degraded and replaced by TCR-CD3 complexes. Due to low levels of CD3 the native TCR outcompetes the xTCR for CD3 recruitment (C). Finally, only native TCR is expressed on the surface, while the xTCR accumulates intracellularly (D).

Though plausible by literature, this effect has not been previously described and remains speculative. To prove this, further experiments need to be conducted, such as immunoprecipitation of xTCR and CD3 subunits.

Following this hypothesis, the process of declining xTCR surface expression would happen particularly fast, if xTCR gets internalized at a higher rate, than the native TCR. However, when adding additional disulfide bonds to the xTCR

no stabilization of surface expression was observed. Suggesting that the kinetic of internalization is not influenced by disulfide linking of TCR chains.

7.6 Elbow region and intrachain domain interactions

To gain further insight into the mechanisms of TCR assembly and surface translocation, we conducted further literature research on TCR structure. As it turns out, there are significant differences in the tertiary and quaternary structure of TCR as opposed to immunoglobulins. Despite being homologous for a large part of their structure (Boulot et al. 1994), there are regions that show very distinct features: In 1995 the structure of the TCR β-chain was unraveled through crystallography (Bentley et al. 1995). It turned out, that while the vβ domain was highly homologous with the v_L domain, the cβ domain showed a more polarized surface. The most significant difference appeared to be the interaction of the variable and constant domain within the β-chain. There was a lot of covered surface area and close interaction between the domains. It was also described that the elbow region of the β-chain would hence be very rigid and lack flexibility.

Also we discovered that a similar approach had been tried before: In 1993 Casorati et al. performed what they described as “αβ V-J domain shuffling” (Casorati 1993). In their approach, they used the TCR derived from the mouse T helper hybridoma 16.2.D, which is an influenza (H1N1) specific TCR. The TCR chains created were of the structure V_α-C_β and V_β-C_α respectively. The transduction was performed in TCR-deficient 58αβ$^-$ hybridoma cell lines. Four double-transductions were performed:

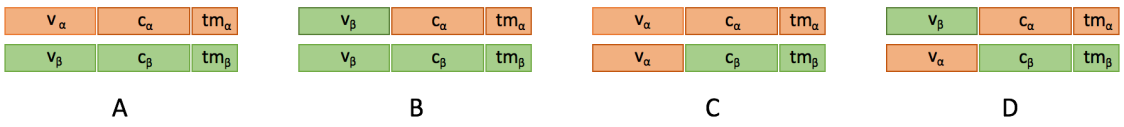

Figure 27: Double transductions performed by Casorati et al.: Vα-Cα and Vβ-Cβ (A), Vβ-Cα and Vβ Cβ (B), Vα-Cα and Vα-Cβ (C), Vβ-Cα and Vα-Cβ (D).

Some of their results align with what we saw in our approach: Except in the unmodified double-transduction, no surface expression was achieved, but they

saw intracellular accumulation. They also performed co-precipitation, proving that there was no intracellular assembly of “shuffled” TCR.

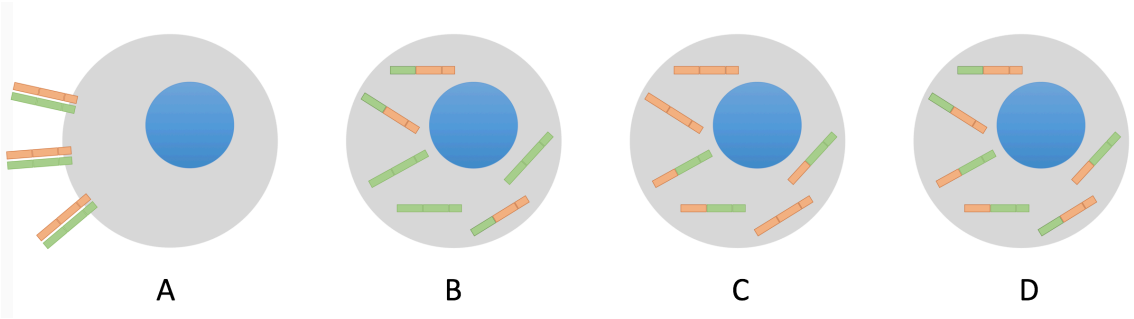

Figure 28: Expression results from Casorati et al.: Except the unmodified TCR (A), no other double transductions yielded TCR surface expression (B-D)

In our approach, however we observed some translocation to the surface, suggesting, that these results do not uniformly apply to all TCR types and domain crossing points. As it appeared that at least to some extent the rigidity of the elbow was responsible for their observations, we reasoned that the exact location of the domain switch within the elbow region might be crucial.

In a final approach, we designed another three constructs with different crossing points in the elbow region, as described in 6.8. While there was no significant improvement of surface expression, there was also no loss thereof. This indicates, that at least in our model, the domain switch approach is somewhat robust to changing the location of the crossing point. However, despite many modifications, we were unable to achieve durable surface expression of xTCR chains.

Due to the partial discrepancy between results in literature and our results, the question arises whether possibly certain subtypes of TCR allow for domain crossings while others do not. To further investigate this, additional TCR crossing would need to be performed and their surface expression assessed.

7.7 Domain-swapped T cell receptors

Recently a similar approach to modifying TCR was published (Bethune et al. 2016). Instead of choosing a domain switch of variable or constant domain, the following three domain switches were used:

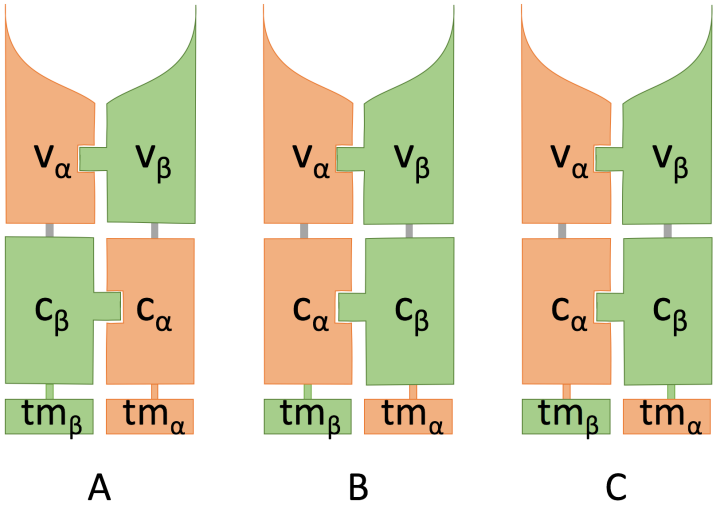

Figure 29: Domain switches used by Bethune et al.: Domain switch at the V-C junction (A), domain switch at the junction between constant domain and transmembrane domain connecting peptide (B) and domain switch at the junction between connecting peptide and transmembrane domain (C).

While the first approach (Figure 29 A) matches our xTCR varia approach, the other two are distinct (Figure 29 B and Figure 29 C). The given publication describes that surface expression was only achieved in the latter two approaches while the first approach failed. These two “domain swapped TCR” (dsTCR) not only showed avidity in dextramer staining, but also retained functional capacity *in vivo*: OT-I dsTCR transduced T cells were able to reject an ovalbumin overexpressing thymoma line when injected into mice in the same way T cells transduced with the unmodified OT-I TCR did. Furthermore, dsTCR chains did not show surface expression when only one dsTCR chain was co-transduced with an unmodified TCR chain into Jurkat T cells. To also exclude mispairing with other native TCR, dsTCR chains were labeled with an N-terminal myc and V5-tag respectively. Then single chains were transduced into primary T cells and detectability of the tags was measured. Tagged unmodified TCR chains showed surface expression due to mispairing, however no surface expression of the tags was detected when using dsTCR chains, proving that mispairing does not occur even when there is a broad variety of native TCR chains to pair with.

Finally, the given publication used the TI-GVHD model described in 3 (Bendle et al. 2010) to examine dsTCR in an *in vivo* mispairing model. In concordance with

the other results, OT-I dsTCR transduced T cells did not cause auto reactivity as seen with unmodified OT-I TCR transduced T cells.

Furthermore, the dsTCR approach was validated with a variety of different TCR, showing that the concept is easily applicable to a wide range of TCR without further adjustments.

However, some limitations to the dsTCR model were also seen: Often the surface expression of dsTCR was significantly lower than that of the unmodified TCR. Bethune et al. reasoned, that the native TCR “outcompete the dsTCR for CD3 recruitment”. To optimize this, they showed that when co-transducing with shRNA (Bunse et al. 2014), they could significantly increase surface expression by decreasing the level of endogenous TCR. The publication also argues that as the switching domains at the V-C junction might improve pairing properties with CD3 as the constant domains would not be switched relatively to the transmembrane domains. However, they state that despite this being possible in antibodies (Schaefer et al. 2011), this attempt fails in TCR in concordance with what we observed in our xTCR approach.

7.8 Conclusions and outlook

Despite different attempts, we were unable to achieve stable surface expression of xTCR. However, we could clearly show that the varia xTCR shows temporary surface expression. Our results in combination with the data of Bethune et al. summarized in the previous chapter, give convincing evidence for domain crossing to successfully prevent mispairing and its detrimental side effects.

Bethune et al. have furthermore shown that when crossing the transmembrane domain instead of variable or constant domain that surface expression is consistently achieved through a variety of TCR and that these dsTCR are functional *in vitro* and *in vivo*. Therefore, providing a relevant alternative to currently established TCR modifications such as single chain TCR.

However, an xTCR with a crossed variable domain still remains desirable as it would ensure a more physiological orientation of CD3 subunit assembly (Bethune et al. 2016). Especially, as the detailed consequences of crossing transmembrane domains on TCR signaling are unknown and the potential side effects of ACT are potent and dangerous (Schumacher 2002, Riechelmann et al. 2007).

It remains unclear, however, whether the xTCR approach described in this thesis is feasible or not. To further assess feasibility, further investigation on structure and pairing properties of xTCR are needed, which require techniques such as protein crystallography and immunoprecipitation. Yet, such techniques were beyond the scope of this thesis, where the aim was a basic characterization of xTCR.

In light of the growing importance and efficacy of ACT, it becomes increasingly relevant to improve the safety of this therapy. For gtACT to move beyond a last line approach, it is imperative to have a repertoire of safe TCR modifications at disposal. The development and further examination of crossed or “domain swapped” TCR is a decisive step in this direction.

8 References

Antony, P.A., Piccirillo, C.A., Akpinarli, A., Finkelstein, S.E., Speiss, P.J., Surman, D.R., Palmer, D.C., Chan, C.C., Klebanoff, C.A., Overwijk, W.W., Rosenberg, S.A. and Restifo, N.P.: CD8+ T cell immunity against a tumor/self-antigen is augmented by CD4+ T helper cells and hindered by naturally occurring T regulatory cells.
The Journal of Immunology, 2005, 5, 2591-2601

Barclay, A.N.: Membrane proteins with immunoglobulin-like domains - A master superfamily of interaction molecules.
Seminars in Immunology, 2003, 4, 215-223

Bendle, G.M., Haanen, J.B.A.G. and Schumacher, T.N.M.: Preclinical development of T cell receptor gene therapy.
Current Opinion in Immunology, 2009, 2, 209-214

Bendle, G.M., Linnemann, C., Hooijkaas, A.I., Bies, L., de Witte, M.a., Jorritsma, A., Kaiser, A.D.M., Pouw, N., Debets, R., Kieback, E., Uckert, W., Song, J.-Y., Haanen, J.B.a.G. and Schumacher, T.N.M.: Lethal graft-versus-host disease in mouse models of T cell receptor gene therapy.
Nature Medicine, 2010, 5, 565-570, 561p following 570

Bentley, G.A., Boulot, G., Karjalainen, K. and Mariuzza, R.A.: Crystal structure of the beta chain of a T cell antigen receptor.
Science, 1995, 5206, 1984-1987

Bethune, M.T., Gee, M.H., Bunse, M., Lee, M.S., Gschweng, E.H., Pagadala, M.S., Zhou, J., Cheng, D., Heath, J.R., Kohn, D.B., Kuhns, M.S., Uckert, W. and Baltimore, D.: Domain-swapped T cell receptors improve the safety of TCR gene therapy.
eLife, 2016, 1-24

Bonifacino, J.S., Cosson, P. and Klausner, R.D.: Colocalized transmembrane determinants for ER degradation and subunit assembly explain the intracellular fate of TCR chains.
Cell, 1990, 3, 503-513

Bonifacino, J.S., Suzuki, C.K. and Klausner, R.D.: A peptide sequence confers retention and rapid degradation in the endoplasmic reticulum.
Science, 1990, 4938, 79-82

Bonifacino, J.S., Suzuki, C.K., Lippincott-Schwartz, J., Weissman, A.M. and Klausner, R.D.: Pre-Golgi degradation of newly synthesized T cell antigen receptor chains: intrinsic sensitivity and the role of subunit assembly.
The Journal of Cell Biology, 1989, 1, 73-83

Boulot, G., Bentley, G.A., Karjalainen, K. and Mariuzza, R.A.: Crystallization and preliminary X-ray diffraction analysis of the beta-chain of a T cell antigen receptor.
Journal of Molecular Biology, 1994, 2, 795-797

Bunse, M., Bendle, G.M., Linnemann, C., Bies, L., Schulz, S., Schumacher, T.N. and Uckert, W.: RNAi-mediated TCR knockdown prevents autoimmunity in mice caused by mixed TCR dimers following TCR gene transfer.
Molecular Therapy, 2014, 11, 1-9

Call, M.E., Pyrdol, J., Wiedmann, M. and Wucherpfennig, K.W.: The organizing principle in the formation of the T cell receptor-CD3 complex.
Cell, 2002, 7, 967-979

Casorati, G.: The T cell receptor alpha beta V-J shuffling shows lack of autonomy between the combining site and the constant domain of the receptor chains.
European Journal of Immunology, 1993, 2, 586-589

Cohen, C.J., Li, Y.F., El-Gamil, M., Robbins, P.F., Rosenberg, S.A. and Morgan, R.A.: Enhanced antitumor activity of T cells engineered to express T cell receptors with a second disulfide bond.
Cancer Research, 2007, 8, 3898-3903

Cohen, C.J., Zhao, Y., Zheng, Z., Rosenberg, S.A. and Morgan, R.A.: Enhanced antitumor activity of murine-human hybrid T cell receptor (TCR) in human lymphocytes is associated with improved pairing and TCR/CD3 stability.
Cancer Research, 2006, 17, 8878-8886

de Witte, M.A., Jorritsma, A., Kaiser, A., van den Boom, M.D., Dokter, M., Bendle, G.M., Haanen, J.B.A.G. and Schumacher, T.N.M.: Requirements for effective antitumor responses of TCR transduced T cells.
The Journal of Immunology, 2008, 7, 5128-5136

Dougan, M. and Dranoff, G.: Immune therapy for cancer.
Annual Review of Immunology, 2009, 83-117

Dudley, M.E., Wunderlich, J.R. and Robbins, P.F.: Cancer Regression and Autoimmunity in Patients After Clonal Repopulation with Antitumor Lymphocytes.
Science, 2002, 5594, 850-854

Dudley, M.E., Yang, J.C., Sherry, R., Hughes, M.S., Royal, R., Kammula, U., Robbins, P.F., Huang, J., Citrin, D.E., Leitman, S.F., Wunderlich, J., Restifo, N.P., Thomasian, A., Downey, S.G., Smith, F.O., Klapper, J., Morton, K., Laurencot, C., White, D.E. and Rosenberg, S.A.: Adoptive cell therapy for patients with metastatic melanoma: Evaluation of intensive myeloablative chemoradiation preparative regimens.
Journal of Clinical Oncology, 2008, 32, 5233-5239

Engels, B. and Uckert, W.: Redirecting T lymphocyte specificity by T cell receptor gene transfer--a new era for immunotherapy.
Molecular Aspects of Medicine, 2007, 1, 115-142

Ferrone, S. and Marincola, F.M.: Loss of HLA class I antigens by melanoma cells: molecular mechanisms, functional significance and clinical relevance.
Immunology Today, 1995, 10, 487-494

Gattinoni, L., Finkelstein, S.E., Klebanoff, C.A., Antony, P.A., Palmer, D.C., Spiess, P.J., Hwang, L.N., Yu, Z., Wrzesinski, C., Heimann, D.M., Surh, C.D., Rosenberg, S.A. and Restifo, N.P.: Removal of homeostatic cytokine sinks by lymphodepletion enhances the efficacy of adoptively transferred tumor-specific CD8+ T cells.
Journal of Experimental Medicine, 2005, 7, 907-912

Govers, C., Sebestyen, Z., Coccoris, M., Willemsen, R.A. and Debets, R.: T cell receptor gene therapy: strategies for optimizing transgenic TCR pairing.
Trends in Molecular Medicine, 2010, 2, 77-87

Heemskerk, M.H.M., Hagedoorn, R.S., Van Der Hoorn, M.A.W.G., Van Der Veken, L.T., Hoogeboom, M., Kester, M.G.D., Willemze, R. and Falkenburg, J.H.F.: Efficiency of T-cell receptor expression in dual-specific T cells is controlled by the intrinsic qualities of the TCR chains within the TCR-CD3 complex.
Blood, 2007, 1, 235-243

Hughes, M.S., Yu, Y.I.K.Y.L., Dudley, M.E., Zheng, Z., Robbins, P.F., Li, Y., Wunderlich, J., Hawley, R.G., Moayeri, M., Rosenberg, S.A. and Morgan, R.A.: Transfer of a TCR Gene Derived from a Patient with a Marked Antitumor Response Conveys Highly Active T-Cell Effector Functions.
Human Gene Therapy, 2005, April, 457-472

Jorritsma, A., Gomez-Eerland, R., Dokter, M., Van De Kasteele, W., Zoet, Y.M., Doxiadis, I.I.N., Rufer, N., Romero, P., Morgan, R.A., Schumacher, T.N.M. and Haanen, J.B.A.G.: Selecting highly affine and well-expressed TCRs for gene therapy of melanoma.
Blood, 2007, 10, 3564-3572

Kim, J.H., Lee, S.-R., Li, L.-H., Park, H.-J., Park, J.-H., Lee, K.Y., Kim, M.-K., Shin, B.A. and Choi, S.-Y.: High cleavage efficiency of a 2A peptide derived from porcine teschovirus-1 in human cell lines, zebrafish and mice.
PLoS One, 2011, 4, e18556-e18556

Klausner, R.D., Lippincott-Schwartz, J. and Bonifacino, J.S.: The T cell antigen receptor: insights into organelle biology.
Annual Review of Cell Biology, 1990, 403-431

Kmieciak, M., Basu, D., Payne, K.K., Toor, A., Yacoub, A., Wang, X.-Y., Smith, L., Bear, H.D. and Manjili, M.H.: Activated NKT cells and NK cells render T cells resistant to myeloid-derived suppressor cells and result in an effective adoptive cellular therapy against breast cancer in the FVBN202 transgenic mouse.
The Journal of Immunology, 2011, 2, 708-717

Kobold, S., Grassmann, S., Chaloupka, M., Lampert, C., Wenk, S., Kraus, F., Rapp, M., Duwell, P., Zeng, Y., Schmollinger, J.C., Schnurr, M., Endres, S. and Rothenfusser, S.: Impact of a new fusion receptor on PD-1-mediated immunosuppression in adoptive T cell therapy.
Journal of the National Cancer Institute, 2015, 8, djv146-djv146

Kuball, J., Dossett, M.L., Wolfl, M., Ho, W.Y., Voss, R.H., Fowler, C. and Greenberg, P.D.: Facilitating matched pairing and expression of TCR chains introduced into human T cells.
Blood, 2007, 6, 2331-2338

Labrecque, N., Whitfield, L.S., Benoist, C. and Mathis, D.: How much TCR does a T cell need?
Immunity, 2001, 1, 71-82

Leisegang, M., Engels, B., Meyerhuber, P., Kieback, E., Sommermeyer, D., Xue, S.-A., Reuss, S., Stauss, H. and Uckert, W.: Enhanced functionality of T cell receptor-redirected T cells is defined by the transgene cassette.
Journal of Molecular Medicine, 2008, 5, 573-583

Maeurer, M.J., Gollin, S.M., Martin, D., Swaney, W., Bryant, J., Castelli, C., Robbins, P., Parmiani, G., Storkus, W.J. and Lotze, M.T.: Tumor escape from immune recognition.
Journal of Clinical Investigation, 1996, 7, 1633-1641

Merhavi-Shoham, E., Haga-Friedman, A. and Cohen, C.J.: Genetically modulating T cell function to target cancer.
Seminars in Cancer Biology, 2012, 1, 14-22

Milstein, C. and Cuello, A.C.: Hybrid hybridomas and their use in immunohistochemistry.
Nature, 1983, 5934, 537-540

Morita, S., Kojima, T. and Kitamura, T.: Plat-E: an efficient and stable system for transient packaging of retroviruses.
Gene Therapy, 2000, 12, 1063-1066

Ochsenbein, A.F., Klenerman, P., Karrer, U., Ludewig, B., Pericin, M., Hengartner, H. and Zinkernagel, R.M.: Immune surveillance against a solid tumor fails because of immunological ignorance.
Proceedings of the National Academy of Sciences, 1999, 5, 2233-2238

Payne, K.K., Toor, A.a., Wang, X.-Y. and Manjili, M.H.: Immunotherapy of cancer: reprogramming tumor-immune crosstalk.
Clinical and Developmental Immunology, 2012, i, 760965-760965

Pedrazzoli, P., Comoli, P., Montagna, D., Demirer, T. and Bregni, M.: Is adoptive T cell therapy for solid tumors coming of age?
Bone Marrow Transplantation, 2012, 8, 1013-1019

Restifo, N.P., Dudley, M.E. and Rosenberg, S.A.: Adoptive immunotherapy for cancer: harnessing the T cell response.
Nature Reviews Immunology, 2012, 4, 269-281

Restifo, N.P., Marincola, F.M., Kawakami, Y., Taubenberger, J., Yannelli, J.R. and Rosenberg, S.A.: Loss of functional beta 2-microglobulin in metastatic melanomas from five patients receiving immunotherapy.
Journal of the National Cancer Institute, 1996, 2, 100-108

Riechelmann, H., Wiesneth, M., Schauwecker, P., Reinhardt, P., Gronau, S., Schmitt, A., Schroen, C., Atz, J. and Schmitt, M.: Adoptive therapy of head and neck squamous cell carcinoma with antibody coated immune cells: a pilot clinical trial.
Cancer Immunology Immunotherapy, 2007, 9, 1397-1406

Rosenberg, S.A., Packard, B.S., Aebersold, P.M., Solomon, D., Topalian, S.L., Toy, S.T., Simon, P., Lotze, M.T., Yang, J.C. and Seipp, C.A.: Use of tumor-infiltrating lymphocytes and interleukin-2 in the immunotherapy of patients with metastatic melanoma. A preliminary report.
New England Journal of Medicine, 1988, 25, 1676-1680

Rosenberg, S.A., Yang, J.C., Sherry, R.M., Kammula, U.S., Hughes, M.S., Phan, G.Q., Citrin, D.E., Restifo, N.P., Robbins, P.F., Wunderlich, J.R., Morton, K.E., Laurencot, C.M., Steinberg, S.M., White, D.E. and Dudley, M.E.: Durable complete responses in heavily pretreated patients with metastatic melanoma using T-cell transfer immunotherapy.
Clinical Cancer Research, 2011, 13, 4550-4557

Sadelain, M., Rivière, I. and Brentjens, R.: Targeting tumours with genetically enhanced T lymphocytes.
Nature Reviews Cancer, 2003, 1, 35-45

Schaefer, W., Regula, J.T., Bähner, M., Schanzer, J., Croasdale, R., Dürr, H., Gassner, C., Georges, G., Kettenberger, H., Imhof-Jung, S., Schwaiger, M., Stubenrauch, K.G., Sustmann, C., Thomas, M., Scheuer, W. and Klein, C.: Immunoglobulin domain crossover as a generic approach for the production of bispecific IgG antibodies.
Proceedings of the National Academy of Sciences, 2011, 27, 11187-11192

Schumacher, T.N.M.: T cell receptor gene therapy.
Nature Reviews Immunology, 2002, 7, 512-519

Sebestyen, Z., Schooten, E., Sals, T., Zaldivar, I., San Jose, E., Alarcon, B., Bobisse, S., Rosato, A., Szollosi, J., Gratama, J., Willemsen, R. and Debets, R.: Human TCR that incorporate CD3zeta induce highly preferred pairing between TCRalpha and beta chains following gene transfer.
The Journal of Immunology, 2008, 11, 7736-7746

Szymczak, A.L. and Vignali, D.a.a.: Development of 2A peptide-based strategies in the design of multicistronic vectors.
Expert Opinion on Biological Therapy, 2005, 5, 627-638

Uckert, W. and Schumacher, T.N.M.: TCR transgenes and transgene cassettes for TCR gene therapy: Status in 2008.
Cancer Immunology, Immunotherapy, 2009, 5, 809-822

Valitutti, S., Müller, S., Salio, M. and Lanzavecchia, A.: Degradation of T Cell Receptor TCR-CD3-ζ Complexes after Antigenic Stimulation.
Journal of Experimental Medicine, 1997, 10, 1859-1864

Willemsen, R.A., Weijtens, M.E., Ronteltap, C., Eshhar, Z., Gratama, J.W., Chames, P. and Bolhuis, R.L.: Grafting primary human T lymphocytes with cancer-specific chimeric single chain and two chain TCR.
Gene Therapy, 2000, 16, 1369-1377

Woods, N.B., Muessig, A., Schmidt, M., Flygare, J., Olsson, K., Salmon, P., Trono, D., Von Kalle, C. and Karlsson, S.: Lentiviral vector transduction of NOD/SCID repopulating cells results in multiple vector integrations per transduced cell: Risk of insertional mutagenesis.
Blood, 2003, 4, 1284-1289

Wu, R., Chacon, J., Bernatchez, C., Haymaker, C., Chen, J.Q., Hwu, P. and Radvanyi, L.G.: Adoptive T cell therapy using autologous tumor-infiltrating lymphocytes for metastatic melanoma: Current status and future outlook.
Cancer Journal, 2012, 2, 160-175

Zhang, T., He, X., Tsang, T.C. and Harris, D.T.: Transgenic TCR expression: comparison of single chain with full-length receptor constructs for T cell function.
Cancer Gene Therapy, 2004, 7, 487-496

9 Appendix

9.1 List of abbreviations

ACT	Adoptive cell therapy
CD3x	CD3 subunit x
CDx	Cluster of differentiation number x
Cα	Constant alpha domain
Cβ	Constant beta domain
DMEM	Dulbecco's Modified Eagle's medium
DMSO	Dimethyl sulfoxide
DNA	Deoxyribonucleic acid
dsTCR	Domains swapped TCR
FBS	Fetal bovine serum
g	Gram or gravity of earth
gtACT	Gene transfer-based adoptive cell therapy
HEPES	4-(2-hydroxyethyl)-1-piperazineethanesulfonic acid
IL-x	Interleukin number x
kb	Kilobase pairs
l	Liter
LB	Lysogeny broth
M	Molar
MDSC	Myeloid-derived suppressor cells
MHC I	Major histocompatibility complex class I
min	Minutes
mol	Mole (unit)
OT-I TCR	MHC class I-restricted, ovalbumin-specific TCR
PBS	Phosphate-buffered saline
PCR	Polymerase chain reaction
RPMI 1640	Roswell Park Memorial Institute medium
TAE	TRIS-Acetate-EDTA
TBI	Total body irradiation
TCR	T cell receptor
TCRα	TCR alpha chain

TCRβ	TCR beta chain
TI-GVHD	TCR gene transfer-induced graft-versus-host disease
TIL	Tumor infiltrating lymphocyte
TM	Transmembrane domain
U	Units
V	Volts
v_H	Variable heavy chain domain
v_L	Variable light chain domain
Vα	Variable alpha domain
Vβ	Variable beta domain
xTCR	Cross TCR

9.2 Acknowledgements

First of all, I would like to thank my doctoral supervisor Professor Stefan Endres who has guided me through my research and who has made this work possible. Next to being a knowledgeable and very experienced researcher, he is the kind of personal mentor any doctoral student can hope for. His great interest and passion for both his work and his doctoral students are qualities that have inspired me and which I hope to possess myself one day.

Then, I want to express my gratitude to PD Sebastian Kobold, who has walked with me every step of the way during this research project. His counsel and guidance combined with his insight and sharp mind, have demonstrated to me how discussion and exchange of thoughts can propel research forward in a way, one could not achieve alone.

I would also like to thank every single member of the laboratory. Those that make our lab a place of smiles and laughter and those that pick you up when one failure chases the next. I have learnt that good research not only requires smart but also good and caring people, who create an atmosphere that allows for personal exchange, just as much as it does for a scientific one, as it is this atmosphere that lets you persevere and overcome any obstacle.

I would also like to mention our partners from Roche, Dr. Claudio Sustman, Dr. Gerhard Niederfellner and Dr. Christian Klein who provided the xTCR vectors and their design and thank them for their close collaboration along the way.

I thank my family for their continuous and unwavering support and advice, not only during my research but throughout my entire life. The backup of my loving family is a force that allows me to chase my dreams and achieve my goals.

And finally, I want to thank my girlfriend Sabine, who has endured every setback just as much as I had to and has never complained. She has given me her advice throughout my entire research and took up the tedious work of proofreading this dissertation.

Eidesstattliche Versicherung

Peters, Philipp

Name, Vorname

Ich erkläre hiermit an Eides statt,

dass ich die vorliegende Dissertation mit dem Thema

T cell receptor modification by alpha and beta chain domain cross-over for adoptive T cell therapy

selbständig verfasst, mich außer der angegebenen keiner weiteren Hilfsmittel bedient und alle Erkenntnisse, die aus dem Schrifttum ganz oder annähernd übernommen sind, als solche kenntlich gemacht und nach ihrer Herkunft unter Bezeichnung der Fundstelle einzeln nachgewiesen habe.

Ich erkläre des Weiteren, dass die hier vorgelegte Dissertation nicht in gleicher oder in ähnlicher Form bei einer anderen Stelle zur Erlangung eines akademischen Grades eingereicht wurde.

München, 06.02.2019

Ort, Datum

Philipp Peters

Unterschrift Doktorandin/Doktorand